Response to Reviewer 1

We thank the reviewer for their helpful comments.

This work investigates the changing fate of atmospheric nitrogen oxides (NOx), with a focus on the increasing importance of the role of organic nitrates. The authors develop a framework by which the fate of NOx can be interpreted using the ratio of contributions to the hydroxyl radical loss rate from nitrogen dioxide and volatile organic hydrocarbons (VOC). The method is then demonstrated using observations from 13 separate field studies, predominantly in the US, dating back over the previous 20 years. The authors then use the framework to investigate the changing role of organic nitrates in the continental US, and the implications for air quality policy. This results in some interesting and important conclusions about the future of NOx chemistry in the US. This is an interesting approach to the study of the non-linear sensitivities of atmospheric NOx chemistry and provides another way by which to explore the importance and impacts of high and low NOx chemical regimes. The approach will also likely prove to be a useful tool for assessing model organic nitrates and responses to changing emissions. The paper is well written and represents a valuable contribution to the literature. I recommend publication after the following comments have been addressed.

Comments:

1) Figure 2 is a very powerful and novel presentation of historical field observations, and warrants more discussion. The authors use of a fit function of the same form as eqn. 4 is convenient for the purposes of this study, but it would be useful to the reader to know the form of a best fit function to the observational data.

In the course of our analysis we have tested several different methods of fitting the data shown in Fig. 2. Multiple forms, including the one presented in Fig. 2, had similar ability to explain the observations (as measured by r^2 or by the standard deviation of the residuals), with no fit clearly superior to the rest. The form presented in Fig. 2 was chosen to be the focus of further analysis both because it matches our theoretical understanding of the process and because it corresponds to a linear relationship between NO2R/VOCR and P(RONO2)/P(HNO3) on a log-log scale. We have added text describing these points:

Page 6: "Despite spanning a large range of environments, all 13 campaigns are well described by a single function of the form $(1 + b \cdot (\mathrm{NO2R/VOCR})^{m})^{-1}$ (red line in Fig. 3a). This functional form corresponds to a linear relationship between $P(RONO_2)/P(HNO_3)$ and NO2R/VOCR on a log-log scale. If m is fixed to 1, then this form also corresponds to the expected behavior if the VOC mixture did not change between environments, and so all parameters other than NO2R/VOCR remained constant (gray line in Fig. 3a)."

The delay seen in the shift from inorganic to organic nitrate dominated NOx loss, as NO2R/VOCR decreases, compared with the best fit line and that predicted by the authors using a fixed VOC speciation (gray line in Fig. 2a) is interesting. This discrepancy occurs at the transition between the high and low NOx regimes identified, i.e. inorganic vs organic nitrate production dominated, and is thus the most important region to understand. It is suggested by the authors that this discrepancy is likely due a change in the effective branding ratio of organic nitrate production (page 5 line 28), however this needs to be supported. Could it not also be due to a change in the reactivity of the VOC mixture, and therefore VOCR, or changes in fNO? The authors should discuss further the observational trends shown in Fig. 2, and the possible explanations for the discrepancy with the simple fit shown in the red line and with the calculated gray line in Fig. 2a. The authors should also comment on the implications of this discrepancy for the conclusions of the paper.

While changes in the VOC mixture do have an importance effect on VOCR, we have already taken this into account in our analysis through the use of NO2R/VOCR as our x-variable. Therefore, changes in the VOC mixture cannot explain the deviations between the observations and the best-fit line. Changes in any of fNO, YRO2, or alpha are a more likely explanation for the discrepancies. We have revised our discussion to discuss this point and included an additional figure showing how all three of these parameters vary with NO2R/VOCR:

Page 8: "While the fraction of NO_x loss occurring via $RONO_2$ chemistry can be well predicted from just the NO2R/VOCR ratio, the observations exhibit a sharper transition from HNO_3-dominated to $RONO_2$-dominated NO_x loss than would be expected if the VOC mixture remained constant. This effect can be explained by variation in $Y_{RO_2\,eff}$, α_{eff}, and $f_{NO_{eff}}$ as NO2R/VOCR changes. The behavior of these three parameters is shown in Fig. 4. As NO2R/VOCR decreases, $f_{NO_{eff}}$ consistently decreases from 0.8 to 0.2, due almost entirely to the decrease in NO_x concentrations. In contrast, both $Y_{RO_2\,eff}$ and α_{eff} are larger in areas with low NO2R/VOCR ratios, due to changes in the VOC mixture between environments. In areas where NO2R/VOCR is high, many of the predominant VOCs, including CO, HCHO, and aromatics, either do not produce RO_2 radicals when oxidized by OH or produce RO_2 radicals that do not efficiently produce organic nitrates, leading to the relatively low values of both these parameters. In areas with low NO2R/VOCR ratios, the VOC mixture is often dominated by biogenic alkenes such as isoprene and monoterpenes that efficiently produce organic nitrates, leading to higher values of both $Y_{RO_{2eff}}$ and α_{eff}. However, although variation in these parameters can help explain some of the observed behavior of fractional NO_x loss, the overall variation is much smaller than the variation of the NO2R/VOCR ratio. Each of the three parameters varies by a factor of 4 or less, while the NO2R/VOCR ratio varies by a factor of 1000."

Figure 4: "VOC oxidation parameters (α_{eff}, $f_{NO_{eff}}$, $Y_{RO_2\,eff}$) as a function of NO2R/VOCR. Used data points are restricted to the continental summer daytime boundary layer (i.e., over land, less than 1.5 km above ground level, and average temperature > 10 °C). The line and solid shapes show the median in each bin, and the vertical lines show an example of the interquartile range for each binned parameter."

2) It would be very useful to the reader to understand how the high and low NOx regimes identified in this work differ from the traditional high to low NOx definition used for describing ozone production regimes (e.g. Jaeglé et al. 1999; Thornton et al. 2002). An important parameter in the traditional conceptual model of high and low NOx chemistry is if the dominant peroxy radical reaction partner is NO or another peroxy radical (i.e. the author defined fNO). In Appendix A the authors have already calculated radical production and loss, and could use this to estimate fNO for each set of observations. It would be helpful for the reader if these values were shown, possibly on Fig. 2a, so the two definitions of high and low NOx chemistries could be compared.

The regimes identified in this paper, of HNO_3-dominated and $RONO_2$-dominated NO_x loss, do not exactly correspond either to the NO_x-saturated/NO_x-limited regimes of ozone production or to the high- NO_x/low-NO_x regimes of peroxy radical chemistry. To avoid confusion, we have removed the terms "high- NO_x" and "low- NO_x " from our manuscript. A graph of fNO is also included in the new Figure 4 in our manuscript.

3) Although the assumptions made in the calculations in Appendix A are commonly used, it is also frequently the case that incomplete measurement suites result in discrepancies with observations. As the authors have radical measurements for some of the field data, comparisons with calculated values for these studies would provide a gauge of the uncertainty in the calculations. The authors should also provide an estimate to which this uncertainty impacts the conclusions of the paper.

All three of the reviewers highlighted the need for additional discussion of the effects of the radical modeling on our results. We have therefore added a section to Appendix A discussing the effects of the steady-state radical modeling on our results:

Page 16: "In order to test the accuracy of the modeling, we used periods when HO_2, OH, and NO were all measured and calculated how the production ratio $P(RONO_2)/P(HNO_3)$ changed if modeled radical concentrations were used instead. These results are shown in Fig. A1. Even in the worst-case scenario (modeled concentrations used for all radicals), the slope is close to one (Fig. A1a), indicating that the use of modeled radicals does not significantly affect our results. Furthermore, Fig A1b–d show that the use of modeled OH or HO_2 concentrations alone does not lead to noticeable changes in $P(RONO_2)/P(HNO_3)$. Use of modeled NO concentrations can cause small but noticeable changes in $P(RONO_2)/P(HNO_3)$, but modeled NO concentrations are used in less than 3% of all data points used in this analysis (238 out of 7988 data points)."

Figure A1: "Comparison of $P(RONO_2)/P(HNO_3)$ when measured concentrations of all possible radicals are used (x-axis) versus when measured concentrations are replaced by modeled concentrations (y-axis). Panel a shows the result when modeled concentrations of OH, HO_2, and NO are all used simultaneously; Panels b–d show the effect of replacing measured with modeled values one species at a time."

4) This work focuses on the daytime production of organic vs inorganic nitrates. Perring et al. (2013), however, estimate that the nocturnal production of organic nitrates, via nitrate radical reactions with alkenes and phenols, could account for as much as 50% of regional production. As NOx and VOC emissions change is the importance of this nocturnal pathway to organic nitrate production also likely to change? A recent analysis by Edwards et al. (2017) presented a similar relationship to that shown here, relating nocturnal organic vs inorganic nitrate formation to the ratio of NOx to VOC, and also predicted a transition from inorganic to organic nitrate dominance. The authors should discuss the role of nocturnal organic nitrate production and how this is accounted for and impacts on the conclusions of this work.

Nighttime oxidation is likely to play an important in the overall rate of NO_x loss. We have performed qualitative analyses that suggest that as the ratio of NO2R/VOCR decreases, $RONO_2$ production is likely to become a greater fraction of nocturnal NO_x loss. However, quantitatively testing these results is extremely difficult for two reasons. First, observations of nighttime chemistry, particularly in the residual layer, are extremely limited, making it hard to examine trends over time. Second, the kinetics of nighttime NO_x chemistry are generally more variable and less well understood than daytime NO_x chemistry. In particular, the value of the reactive uptake coefficient for N_2O_5 on aerosols can vary by several orders of magnitude and is not well predicted by current models, making it difficult to predict how NO_x will be lost in different environments. A more full examination of trends in the nighttime mechanics of NO_x loss is an important topic for further research, but one that we feel is better suited to its own analyses than to be included in this paper.

We have added a section to this paper describing nocturnal NO_x chemistry, the similarities between the daytime and nighttime oxidation mechanisms, and the difficulties of extending the analysis from Fig. 2 into the night:

Page 9: "While the primary focus of this analysis is on daytime chemistry, a conceptually similar transition may also occur at night. At night, OH concentrations are near zero, and the first step in NO_x oxidation is the reaction of NO_2 with O_3 to produce NO_3. This radical can in turn react either with NO_2 to form N_2O_5 or with an alkene to form an organic nitrate (R8 – R9).

$NO_3 + RH \rightarrow RONO_2$ (R8)

$NO_3 + NO_2 \leftrightarrow N_2O_5$ (R9)

Finally, N_2O_5 can either thermally decompose to reform NO_3 and NO_2 or it can hydrolyze on aerosol surfaces to produce HNO_3 (R9 – R10).

$N_2O_5 \xrightarrow{k_{hyd}} 2HNO_3$ (R10)

Although the details of the nighttime chemical system are different, it shares some fundamental similarities with the daytime system: NO_x can be lost through the production of $RONO_2$ or of HNO_3, and a key step controlling the relative importance of these two sinks is whether an oxidant reacts with NO_2 or with a VOC. These similarities suggest that the relative importance of $RONO_2$ and HNO_3 as NO_x sinks at night may also be controlled by the relative reactivities of NO_2 and VOCs towards NO_3. In areas where NO_3 is more likely to react with NO_2, HNO_3 production is likely to dominate NO_x loss, while the opposite is likely to be true in areas where NO_3 is more likely to react with a VOC.

However, quantitatively estimating the relative fraction of NO_x loss through these different pathways is not practical with the combined dataset presented here. There have been relatively few measurement of the nocturnal atmosphere (only 4 of the 13 campaigns in Table 1 include nighttime measurements) and there remain significant uncertainties in the kinetics of nighttime NO_x loss. In particular, the overall rate of N_2O_5 hydrolysis is controlled by the reactive uptake parameter γ and the aerosol surface area, both of which can vary by multiple orders of magnitude (McDuffie et al., 2018; Brown et al., 2009). Variation in the rate of N_2O_5 hydrolysis may therefore also play a major role in controlling the relative importance of $RONO_2$ and HNO_3 production to NO_x loss at night. While developing a more quantitative understanding of the trends in the chemical mechanisms of nocturnal NO_x loss is an important area for future research, the conceptual similarity between the daytime and nighttime regimes suggests that the conclusions drawn here based on the daytime chemistry may also be relevant to the nighttime. "

Response to Reviewer 2

We thank the reviewer for their helpful comments.

This paper evaluated the relative importance of two NOx removal pathways, forming HNO3 and RONO2. The fraction of NOx loss via RONO2 chemistry was approximated the contribution of VOC to the total OH reactivity with additional consideration of RONO2 yield. The comparison of such simple calculation and 13 field campaigns results show consistent trend, which give confidence to conduct long-term prediction. The impact on the ozone production is discussed based on the growing importance of RONO2 chemistry to NOx loss. Finally, the spatial distribution of NOx lifetime is evaluated using WRF-Chem model for the 2013 summer United States. This paper presents an interesting result on the fate of NOx using a simplified but insightful approach. The paper is well written and the method to evaluate the fate the NOx is helpful to diagnose the non-linearity of the atmospheric chemistry. I recommend publication after the following comments are addressed.
Comments:

(1) The uncertainty in the radical budget calculation. In the appendix, the production of OH, HO2 and RO2 are not complete. The HONO photolysis, alkene ozonolysis are missing. How much does the result rely on this budget analysis? Some results showed that HONO photolysis, as an OH source, is more important than ozone photolysis in polluted environments (Mao et al., 2010;Tan et al., 2019). Ozonolysis of alkenes, isoprene, and monoterpenes could be important radical source in forest areas (Griffith et al., 2013). A discussion on this missing radical source and its impact would be helpful.

We have revised our calculation of P(HO_x) to include photolysis of HONO when measurements of HONO are available as well as alkene ozonolysis. The resulting P(HO_x) rates and radical concentrations did not significantly change, suggesting that these radical sources are not large contributors to the radical budget in our dataset. We have revised the manuscript to include these new radical sources in our calculations:

Page 5: "When these radicals were not available, OH, and HO_2 radical concentrations were also calculated iteratively based on the total rate of HO_x radical production by O_3 photolysis, HCHO photolysis, and alkene ozonolysis. When HONO was measured, HONO photolysis was also included as an OH source."

Equation A7:

$$P(\mathrm{OH}) \quad = \quad \frac{2j_{\mathrm{O_3\rightarrow O^1D}}[\mathrm{O_3}]\cdot k_{\mathrm{O^1D+H_2O}}[\mathrm{H_2O}]}{k_{\mathrm{O^1D+H_2O}}[\mathrm{H_2O}]+k_{\mathrm{O^1D}+M}[M]}+j_{\mathrm{HONO}}[\mathrm{HONO}]+k_{\mathrm{HO_2+NO}}[\mathrm{HO_2}][\mathrm{NO}]+k_{\mathrm{O_3+RH}}[\mathrm{O_3}][\mathrm{RH}]Y_{\mathrm{OH}}$$

Furthermore, based on comments from all 3 reviewers, we have added a sensitivity analysis of how the use of modeled radical concentrations affects our results:

Page 16: "In order to test the accuracy of the modeling, we used periods when HO_2, OH, and NO were all measured and calculated how the production ratio $P(RONO_2)/P(HNO_3)$ changed if modeled radical concentrations were used instead. These results are shown in Fig. A1. Even in the worst-case scenario (modeled concentrations used for all radicals), the slope is close to one (Fig. A1a), indicating that the use of modeled radicals does not significantly affect our results. Furthermore, Fig A1b–d show that the use of modeled OH or HO_2 concentrations alone does not lead to noticeable changes in $P(RONO_2)/P(HNO_3)$. Use of modeled NO concentrations can cause small but noticeable changes in $P(RONO_2)/P(HNO_3)$, but modeled NO concentrations are used in less than 3% of all data points used in this analysis (238 out of 7988 data points)."

Figure A1: "Comparison of $P(RONO_2)/P(HNO_3)$ when measured concentrations of all possible radicals are used (x-axis) versus when measured concentrations are replaced by modeled concentrations (y-axis). Panel a shows the result when modeled concentrations of OH, HO_2, and NO are all used simultaneously; Panels b–d show the effect of replacing measured with modeled values one species at a time."

Also, I assume these radical concentrations are used to calculate the P(HNO3) and P(RONO2) separately for each 13 campaigns but it's not clear in the context. The authors should make this point clearer:

Yes, the radical concentrations were calculated separately for each campaign and used to calculate $P(HNO_3)$ and $P(RONO_2)$:

Page 5: "Where available, measurements of OH and HO_2 were used to directly calculate RO_2 formation and loss. When these radicals were not available, OH, and HO_2 radical concentrations were also calculated iteratively based on the total rate of HO_x radical production by O_3 photolysis, HCHO photolysis, and alkene ozonolysis. When HONO was measured, HONO photolysis was also included as an OH source. In a small fraction of cases (3% of all data points), NO measurement are not available and NO concentration were calculated based on the concentrations of O_3 and NO_2. Details of the radical modeling, including the equations used to calculate the production and loss of these radicals, are given in Appendix A. "

*(2) The detail description of alpha. The organic nitrate yield is determined for different VOCs and explained in the appendix. However, I would suggest adding a table to describe the range of organic nitrate yield. As I found in Figure 2, the least- squares fit is y=(1+125x^1.06)^{-1} and 125 should be equal to 1/(alpha*fNO*YRO2), the alpha would be 0.008 if fNO and YRO2 are unity. In this case, a comparison with least-squares fit to Eq. 4 and discussion on the parameters would be helpful to the reader to understand what the meaning of such fit function is.*

We have added an additional figure to the manuscript showing values of alpha, fNO, and YRO2 as a function of NO2R/VOCR, as well as a paragraph describing the variation in these three parameters:

Page 8: "While the fraction of NO_x loss occurring via $RONO_2$ chemistry can be well predicted from just the NO2R/VOCR ratio, the observations exhibit a sharper transition from HNO_3-dominated to $RONO_2$-dominated NO_x loss than would be expected if the VOC mixture remained constant. This effect can be explained by variation in $Y_{RO_{2\,eff}}$, α_{eff}, and $f_{NO_{eff}}$ as NO2R/VOCR changes. The behavior of these three parameters is shown in Fig. 4. As NO2R/VOCR decreases, $f_{NO_{eff}}$ consistently decreases from 0.8 to 0.2, due almost entirely to the decrease in NO_x concentrations. In contrast, both $Y_{RO_{2\,eff}}$ and α_{eff} are larger in areas with low NO2R/VOCR ratios, due to changes in the VOC mixture between environments. In areas where NO2R/VOCR is high, many of the predominant VOCs, including CO, HCHO, and aromatics, either do not produce RO_2 radicals when oxidized by

OH or produce RO_2 radicals that do not efficiently produce organic nitrates, leading to the relatively low values of both these parameters. In areas with low NO2R/VOCR ratios, the VOC mixture is often dominated by biogenic alkenes such as isoprene and monoterpenes that efficiently produce organic nitrates, leading to higher values of both $Y_{RO_{2eff}}$ and α_{eff}. However, although variation in these parameters can help explain some of the observed behavior of fractional NO_x loss, the overall variation is much smaller than the variation of the NO2R/VOCR ratio. Each of the three parameters varies by a factor of 4 or less, while the NO2R/VOCR ratio varies by a factor of 1000."

Figure 4: "VOC oxidation parameters (α_{eff} , $f_{NO_{eff}}$, $Y_{RO_2\,eff}$) as a function of NO2R/VOCR. Used data points are restricted to the continental summer daytime boundary layer (i.e., over land, less than 1.5 km above ground level, and average temperature > 10 °C). The line and solid shapes show the median in each bin, and the vertical lines show an example of the interquartile range for each binned parameter."

(3) Some argumentation are too general or without explanation.

Page 4 Line 23, please define low-NOx

Because the terms low-NO_x and high-NO_x do not have an agreed upon definition and often cause confusion, we have removed these terms from this manuscript:

Page 4: "f_{NO_i} is close to 1 under polluted or moderately-polluted conditions, but decreases as the concentration of NO_x decreases."

Page 9 Line 1-2, according to Fig. 3, this statement relies on an assumption that many regions are located in the transition regime (e.g. NO2R/VOCR ranges from 2e-2 to 1e-3). The authors should provide relevant information to support this argument.

We have added a histogram of showing the number of observations as a function of NO2R/VOCR:

Page 5: "Although these field campaigns do not constitute a random sample of the atmosphere, the combined dataset provides an excellent survey of atmospheric chemistry over a wide range of conditions. The combined dataset includes nearly 8000 data points for which fractional NO_x loss can be calculated, spanning nearly 3 orders of magnitude in the ratio of NO2R to VOCR with no significant gaps (Fig. 2.)"

Figure 2: "Number of points in each bin for which the fraction of NO_x loss occurring via $RONO_2$ chemistry could be calculated."

Page 11: "Given the large number of data points sampled in this transition regime (Fig. 2), many regions of the United States are therefore likely to transition from a regime where HNO_3 dominates NO_x loss to a mixed or $RONO_2$-dominated regime."

Page 9 Line 12, please define comprehensive metric.

We have reworded the sentence to clarify:

Page 11: " When considering ozone pollution on regional scales, OPE is a more appropriate metric than instantaneous ozone production because it accounts for ozone production both locally and further afield. "

Page 5 Line 2, please provide the reaction rate constant for OH+NO2 reaction and the literature

We have added this information to Appendix A:

Page 15: "The reaction rate constant for NO_2 with OH was taken from Mollner et al. (2010), with temperature- and pressure-dependencies from Henderson et al. (2012)."

Technical corrections: Page 5 Line 1, 'NO2R' 2 should be subscripted. Page 9 Line 10, 'P(O3)' 3 should be subscripted. Page 13 Line 14, (A3) 2jHCHO[HCHO] Page 13 Line 19, (A8) L(OH) should be (VOCR+NO2R)*[OH]*

We thank the reviewer for bringing these errors to our attention

Response to Reviewer 3

This referee agrees with what already suggested by the other reviewers. In particular the point regarding the calculation of the OH, HO2 and RO2 and radicals should be better discussed. As pointed out a better analysis of the uncertainties for the calculation should be done together with the inclusion, if possible, of HONO photolysis and ozonolysis of unsaturated compounds. The calculation, as is at the moment, is very simplified (for example, why not including reaction with CO when considering the losses of OH radicals?) and it can well be that it is good enough for this study but a sensitivity check by adding additional sources would help understand their impact. In addition, the comparison, where possible, with the available radical measurements would also help understanding the reliability of the simple calculation used.

We have revised our calculation of $P(\mathrm{HO_x})$ to include photolysis of HONO when measurements of HONO are available as well as alkene ozonolysis. The resulting $P(\mathrm{HO_x})$ rates and radical concentrations did not significantly change, suggesting that these radical sources are not large contributors to the radical budget in our dataset. We have revised the manuscript to include these new radical sources in our calculations:

Page 5: "When these radicals were not available, OH, and HO_2 radical concentrations were also calculated iteratively based on the total rate of HO_x radical production by O_3 photolysis, HCHO photolysis, and alkene ozonolysis. When HONO was measured, HONO photolysis was also included as an OH source."

Equation A7:

$$P(\mathrm{OH}) \quad = \quad \frac{2j_{\mathrm{O_3\rightarrow O^1D}}[\mathrm{O_3}]\cdot k_{\mathrm{O^1D+H_2O}}[\mathrm{H_2O}]}{k_{\mathrm{O^1D+H_2O}}[\mathrm{H_2O}]+k_{\mathrm{O^1D+}M}[M]}+j_{\mathrm{HONO}}[\mathrm{HONO}]+k_{\mathrm{HO_2+NO}}[\mathrm{HO_2}][\mathrm{NO}]+k_{\mathrm{O_3+RH}}[\mathrm{O_3}][\mathrm{RH}]Y_{\mathrm{OH}}$$

Furthermore, based on comments from all 3 reviewers, we have added a sensitivity analysis of how the use of modeled radical concentrations affects our results:

Page 16: "In order to test the accuracy of the modeling, we used periods when HO_2, OH, and NO were all measured and calculated how the production ratio $P(RONO_2)/P(HNO_3)$ changed if modeled radical concentrations were used instead. These results are shown in Fig. A1. Even in the worst-case scenario (modeled concentrations used for all radicals), the slope is close to one (Fig. A1a), indicating that the use of modeled radicals does not significantly affect our results. Furthermore, Fig A1b–d show that the use of modeled OH or HO_2 concentrations alone does not lead to noticeable changes in $P(RONO_2)/P(HNO_3)$. Use of modeled NO concentrations can cause small but noticeable changes in $P(RONO_2)/P(HNO_3)$, but modeled NO concentrations are used in less than 3% of all data points used in this analysis (238 out of 7988 data points)."

Figure A1: "Comparison of $P(RONO_2)/P(HNO_3)$ when measured concentrations of all possible radicals are used (*x*-axis) versus when measured concentrations are replaced by modeled concentrations (*y*-axis). Panel a shows the result when modeled concentrations of OH, HO_2, and NO are all used simultaneously; Panels b–d show the effect of replacing measured with modeled values one species at a time."

Finally, we have revised our explanation of OH reactivity to clarify that loss of OH by reaction with CO is included, as well as the reaction of OH with other compounds that are not included in either VOCR or NO2R:

Page 15: "In (A8), the symbol XR is used to represent the OH reactivity of species such as SO_2 and O_3 that are not included in either VOCR or NO2R. Although it is not often categorized as a VOC, CO is included as a contributor to VOCR."

The changing role of organic nitrates in the removal and transport of NO_x

Paul S. Romer Present[1], Azimeh Zare[1], and Ronald C. Cohen[1,2]

[1]Department of Chemistry, University of California Berkeley, Berkeley, CA, 94720, USA.
[2]Department of Earth and Planetary Sciences, University of California Berkeley, Berkeley, CA, 94720, USA.

Correspondence: Ronald C. Cohen (rccohen@berkeley.edu)

Abstract. A better understanding of the chemistry of nitrogen oxides (NO_x) is crucial to effectively reducing air pollution and predicting future air quality. The response of NO_x lifetime to perturbations in emissions or in the climate system is set in large part by whether NO_x loss occurs primarily by the direct formation of HNO_3 or through the formation of alkyl and multifunctional nitrates ($RONO_2$). Using 15 years of detailed in situ observations, we show that in the ~~summertime~~ summer daytime continental boundary layer the relative importance of these two pathways can be well approximated by the relative likelihood that OH will react with NO_2 or instead with a volatile organic compound (VOC). Over the past decades, changes in anthropogenic emissions of both NO_x and VOCs have led to a significant increase in the overall importance of $RONO_2$ chemistry to NO_x loss. We find that this shift is associated with a decreased effectiveness of NO_x emissions reductions on ozone production in polluted areas and increased transport of NO_x from source to receptor regions. This change in chemistry, combined with changes in the spatial pattern of NO_x emissions, is observed to be leading to a flatter distribution of NO_2 across the United States, potentially transforming ozone air pollution from a local issue into a regional one.

1 Introduction

Nitrogen oxides ($NO_x \equiv NO + NO_2$) play a central role in the formation of toxic air pollutants including O_3 and secondary aerosols. More broadly, NO_x chemistry controls the rates and pathways of atmospheric oxidation by determining the concentration of the three most important tropospheric oxidants: OH, O_3, and NO_3. NO_x emissions also directly contribute to nitrogen deposition in sensitive ecosystems (Fowler et al., 2013). Due to its harmful effects to the environment and human health, NO_x has been the target of emissions control strategies since the 1970s, causing anthropogenic NO_x emissions in the United States to have decreased by a factor of 2 or more over the past 30 years (United States Environmental Protection Agency, 2018). Understanding the consequences of these past changes and predicting the results of future emissions reductions on the atmosphere requires a quantitative description of feedbacks between NO_x concentrations and NO_x chemistry.

After emission to the atmosphere, removal of NO_x occurs through two primary pathways: conversion to HNO_3 and conversion to alkyl and multifunctional nitrates ($RONO_2$). Once formed, HNO_3 is nearly chemically inert in the troposphere, with a lifetime to reaction or photolysis of over 50 hours. HNO_3 is therefore removed almost entirely by wet and dry deposition. $RONO_2$ represents a class of diverse molecules, with atmospheric lifetimes ranging from hours to days depending on the properties of the organic backbone (R-group). The loss of $RONO_2$ is divided among reactions that release NO_x from the R-group and recycle it back to the atmosphere, reactions that result in heterogeneous hydrolysis to form HNO_3, and direct deposition. The latter two pathways permanently remove NO_x from the atmosphere (Nguyen et al., 2015; Romer et al., 2016; Fisher et al., 2016). Other NO_x oxidation products, such as peroxy acetyl nitrate (PAN) or HONO can play an important role in the transport and redistribution of NO_x but do not generally lead to permanent NO_x removal.

Historically, direct HNO_3 production was thought to be the only important NO_x loss pathway, with $RONO_2$ chemistry playing at most a minor role. However, several studies have shown that the formation rate of $RONO_2$ in cities or forested regions can be competitive with or greater than the direct production rate of nitric acid (Rosen et al., 2004; Farmer et al., 2011; Browne et al., 2013; Romer et al., 2016; Sobanski et al., 2017).

The relative importance of HNO_3 and $RONO_2$ production is an important factor in setting the lifetime of NO_x (Romer et al., 2016) and affects the response of NO_x loss to temperature (Romer et al., 2018). Due to their different production pathways, the relative importance of HNO_3 and $RONO_2$ production also controls how NO_x loss and ozone production are affected by changes to emissions of NO_x or volatile organic compounds (VOCs). By terminating the radical chain reactions, the formation of $RONO_2$ serves to suppress ozone formation in polluted areas (Perring et al., 2010; Farmer et al., 2011; Edwards et al., 2013; Lee et al., 2014). Several studies have also shown that $RONO_2$ can efficiently partition into aerosols, potentially explaining a large portion of secondary organic aerosol in a wide range of environments (Rollins et al., 2012; Pye et al., 2015; Xu et al., 2015b; Lee et al., 2016).

Multiple previous studies have used chemical transport models to investigate how the relative production of $RONO_2$ and HNO_3 varies in different environments. Browne and Cohen (2012) modeled NO_x loss over the Canadian Boreal Forest using WRF-Chem and Fisher et al. (2016) and Zare et al. (2018) studied NO_x loss in the southeast United States using GEOS-Chem and WRF-Chem respectively. These studies agree that in rural and forested areas with lower NO_x emissions and higher biogenic VOC emissions, $RONO_2$ chemistry is often the largest sink of NO_x.

However, these studies diverge in their conclusions about the overall importance of $RONO_2$ chemistry as a NO_x sink and how it is likely to change in the future. In a WRF-Chem simulation identical to those described in Zare et al. (2018), $RONO_2$ chemistry is found to be 60 % or more of the total NO_x loss across broad swathes of the southeast United States (Fig. 1), while Fisher et al. (2016) found $RONO_2$ production to be concentrated in rather small sections of the southeast. Furthermore, Fisher et al. (2016) suggested that the contribution of $RONO_2$ chemistry to NO_x loss across the region is unlikely to change significantly in the future due to the spatial segregation of NO_x and VOC emissions. On the other hand, Zare et al. (2018) and Browne and Cohen (2012) suggested that the the contribution of $RONO_2$ chemistry to NO_x loss was likely to grow significantly if anthropogenic NO_x emissions decreased across the United States.

Here we use in situ observations from a collection of 13 different field deployments to investigate how the relative daytime production of $RONO_2$ and HNO_3 varies across the United States and how this fraction may change in the future. We show that the relative production of $RONO_2$ and HNO_3 can be well described by the relative OH reactivity of NO_2 and of the combined VOC mixture. As both anthropogenic NO_x and anthropogenic VOC emissions have decreased substantially in the United States over the past 20 years, the relative role of these two pathways has shifted as well. While the shift has generally

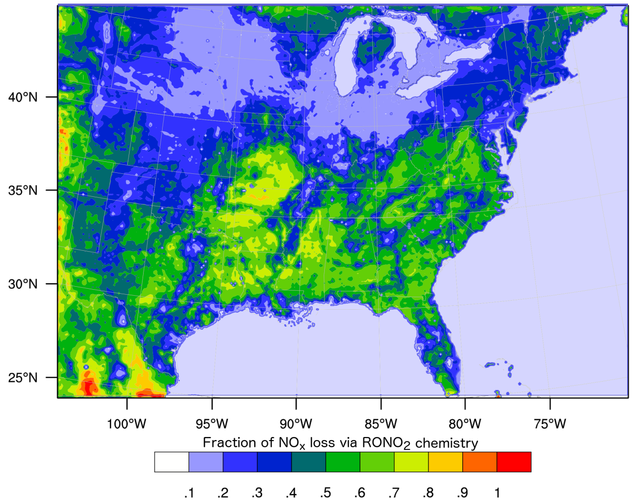

Figure 1. Average (24-hour) fraction of total $\mathrm{NO_x}$ loss via $\mathrm{RONO_2}$ chemistry over the southeast United States in summer 2013 simulated using the RACM2_Berkeley2 mechanism in WRF-Chem (Zare et al., 2018).

been towards an increasing role for $\mathrm{RONO_2}$ chemistry, the shift has been smallest in large cities and largest in the transitional regime around them. Combined with changing emission patterns of $\mathrm{NO_x}$, the shift in $\mathrm{NO_x}$ chemistry is leading to a flatter distribution of $\mathrm{NO_x}$ across the continental United States.

2 $\mathrm{NO_x}$ chemistry and production of $\mathrm{RONO_2}$ and $\mathrm{HNO_3}$

$\mathrm{NO_x}$ is emitted to the atmosphere as NO from a range of anthropogenic and biogenic sources, including motor vehicles, power plants, lightning, fires, and soil bacteria. In the daytime, NO interconverts with $\mathrm{NO_2}$ on a timescale of minutes through Reactions (R1–R2), forming the chemical family $\mathrm{NO_x}$. When $\mathrm{NO_x}$ is combined with VOCs and hydrogen oxides ($\mathrm{HO_x}$), a set of linked radical chain reactions is formed (~~Reactions~~ R3–R6). As part of these reactions, two molecules of NO are oxidized to $\mathrm{NO_2}$, leading to the net production of $\mathrm{O_3}$ through Reaction (R2).

$$\mathrm{NO + O_3 \rightarrow NO_2 + O_2} \qquad \text{(R1)}$$

$$\mathrm{NO_2} + h\nu + \mathrm{O_2 \rightarrow O_3 + NO} \qquad \text{(R2)}$$

$$\mathrm{OH + R + O_2 \rightarrow RO_2 + H_2O} \qquad \text{(R3)}$$

$$\mathrm{RO_2 + NO \xrightarrow{1-\alpha} RO + NO_2} \tag{R4a}$$

$$\mathrm{RO + O_2 \rightarrow R'CHO + HO_2} \tag{R5}$$

$$\mathrm{HO_2 + NO \rightarrow OH + NO_2} \tag{R6}$$

The reactions that propagate the catalytic cycle occur at the same time as reactions that remove $\mathrm{NO_x}$ from the atmosphere, terminating the cycle. Direct $\mathrm{HNO_3}$ production occurs through the association of OH with $\mathrm{NO_2}$ (R7). $\mathrm{RONO_2}$ compounds are produced as a minor channel of the $\mathrm{RO_2 + NO}$ reaction (R4b). Some fraction of the time α, these two radicals will associate to form an organic nitrate, with the balance forming $\mathrm{NO_2}$ and eventually producing $\mathrm{O_3}$ (R4a). The branching ratio $k_{\mathrm{R4b}}/(k_{\mathrm{R4a}} + k_{\mathrm{R4b}})$ is designated α and is determined by the nature of the R group as well as the temperature and pressure. Longer carbon backbones and lower temperatures increase α, while lower pressures and oxygenated functional groups decrease it (Wennberg et al., 2018). Typical values of α in the summertime continental boundary layer range from near 0 for small hydrocarbons and highly oxygenated compounds to over 0.20 for large alkanes and alkenes (Perring et al., 2013).

$$\mathrm{OH + NO_2} + M \rightarrow \mathrm{HNO_3} + M \tag{R7}$$

$$\mathrm{RO_2 + NO} + M \xrightarrow{\alpha} \mathrm{RONO_2} + M \tag{R4b}$$

The total rate of $\mathrm{RONO_2}$ production can be calculated from the properties of individual VOCs measured in the atmosphere via Eq. (1). In Eq. (1), $Y_{\mathrm{RO_2}_i}$ represents the yield of $\mathrm{RO_2}$ radicals from VOC oxidation and f_{NO_i} represents the fraction of those $\mathrm{RO_2}$ radicals that react with NO instead of reacting with $\mathrm{HO_2}$ or undergoing unimolecular isomerization (e.g., Teng et al., 2017). f_{NO_i} is close to 1 under polluted or moderately-polluted conditions, but decreases ~~in low-$\mathrm{NO_x}$ conditions~~as the concentration of $\mathrm{NO_x}$ decreases.

$$P(\mathrm{RONO_2}) = [\mathrm{OH}] \sum_{R_i} [\mathrm{R_i}] \cdot k_{\mathrm{OH+R_i}} \cdot Y_{\mathrm{RO_2}_i} \cdot f_{\mathrm{NO}_i} \cdot \alpha_i \tag{1}$$

If the contributions from individual VOCs are summed and averaged, the total production of $\mathrm{RONO_2}$ can also be calculated from the effective behavior of the VOC mixture via Eq. (2), where VOCR is the sum of all measured VOC concentrations weighted by their reaction rate with OH.

$$P(\mathrm{RONO_2}) = [\mathrm{OH}] \cdot \mathrm{VOCR} \cdot Y_{\mathrm{RO_2}_{\mathrm{eff}}} \cdot f_{\mathrm{NO_{eff}}} \cdot \alpha_{\mathrm{eff}} \tag{2}$$

In a similar fashion, the production of HNO_3 can be calculated via Eq. (3), where NO2R is the NO_2 reactivity, or the concentration of NO_2 multiplied by k_{OH+NO_2}. At 298 K and 1 atm, 10 ppb of NO_2 is equivalent to an NO2R of 2.3 s^{-1}.

$$P(\mathrm{HNO_3}) = [\mathrm{OH}] \cdot [\mathrm{NO_2}] \cdot k_{\mathrm{OH+NO_2}} = [\mathrm{OH}] \cdot \mathrm{NO2R} \tag{3}$$

Total NO_x loss is the sum of the conversion to HNO_3 and conversion to $RONO_2$. The fraction of NO_x loss via $RONO_2$ production can be expressed analytically as Eq. 4.

$$\frac{P(\mathrm{RONO_2})}{P(\mathrm{RONO_2}) + P(\mathrm{HNO_3})} = \left(1 + \frac{1}{\alpha_{\mathrm{eff}} \cdot f_{\mathrm{NO_{eff}}} \cdot Y_{\mathrm{RO_{2eff}}}} \times \frac{\mathrm{NO2R}}{\mathrm{VOCR}}\right)^{-1} \tag{4}$$

The relative production of $RONO_2$ and HNO_3 is seen to be controlled by two factors, the first describing the chemistry of RO_2 radicals (α_{eff}, $f_{\mathrm{NO_{eff}}}$, $Y_{\mathrm{RO_{2eff}}}$), and the second the ratio of NO2R to VOCR, which describes whether OH is more likely to react with a VOC or with NO_2. Because Eq. 4 concerns fractional loss of NO_x, the concentration of OH, which affects $RONO_2$ and HNO_3 production equally, does not appear in the result.

We show below that in the summertime continental boundary layer, the terms describing RO_2 radical chemistry vary significantly less than the NO2R/VOCR ratio, allowing the relative importance of $RONO_2$ and HNO_3 chemistry to be roughly estimated from only a single ratio.

3 Observed contributions of HNO_3 and $RONO_2$ chemistry to NO_x loss

3.1 Daytime chemistry

Relative $RONO_2$ and HNO_3 production rates were calculated for 13 separate campaign deployments in the northern hemisphere over the past 20 years. Campaigns were selected that included measurements of NO_x, HNO_3, O_3, HCHO, a wide range of VOCs, and total organic nitrates ($\Sigma RONO_2$). Although they do not include measurements of $\Sigma RONO_2$, ITCT2k2 and CALNEX-P3 were also included to provide a pair of measurements of VOCs and NO_x in the same geographic location separated in time. A list of all campaigns used in this study is given in Table 1. Where available, measurements of OH and HO_2 were used to directly calculate RO_2 formation and loss~~; when~~. When these radicals were not available, OH, ~~HO_2, and RO_2~~ and HO_2 radical concentrations were also calculated iteratively based on the total rate of HO_x radical production by O_3 ~~and HCHO photolysis. Equations~~ photolysis, HCHO photolysis, and alkene ozonolysis. When HONO was measured, HONO photolysis was also included as an OH source. In a small fraction of cases (3% of all data points), NO measurement are not available and NO concentration were calculated based on the concentrations of O_3 and NO_2. Details of the radical modeling, including the equations used to calculate the production and loss of these radicals, are given in Appendix A.

Although these field campaigns do not constitute a random sample of the atmosphere, the combined dataset provides an excellent survey of atmospheric chemistry over a wide range of conditions. The combined dataset includes nearly 8000 data points for which fractional NO_x loss can be calculated, spanning nearly 3 orders of magnitude in the ratio of NO2R to VOCR with no significant gaps (Fig. 2).

Table 1. Field campaigns used in this analysis

Campaign name	Data Reference	Format	Year	Base of Operations	Date
ITCT2k2	ITCT Science Team (2002)	Airborne	2002	Monterey, CA	22 Apr – 19 May
INTEX-NA	INTEX-A Science Team (2006)	Airborne	2004	Palmdale, CA	2 Jul
				Mascoutah, IL	7 Jul – 14 Jul
				Portsmouth, NH	16 Jul – 10 Aug
				Mascoutah, IL	12 Aug
INTEX-B	INTEX-B Science Team (2011)	Airborne	2006	Houston, TX	4 Mar – 19 Mar
				Honolulu, HI	23 Apr – 28 Apr
				Anchorage, AK	1 May – 12 May
BEARPEX 2007	BEAPREX 07 Science Team (2007)	Ground	2007	Georgetown, CA	15 Aug –10 Oct
ARCTAS-B	ARCTAS-B Science Team (2011)	Airborne	2008	Palmdale, CA	18 Jun – 24 Jun
				Cold Lake, Alberta, CAN	29 Jun – 8 Jul
				Thule, Greenland	8 Jul – 10 Jul
BEARPEX 2009	BEAPREX 09 Science Team (2009)	Ground	2009	Georgetown, CA	15 Jun – 31 Jul
CALNEX-P3	CALNEX Science Team (2002a)	Airborne	2010	Ontario, CA	1 May – 22 Jun
CALNEX-SJV	CALNEX Science Team (2002b)	Ground	2010	Bakersfield, CA	15 May – 30 Jun
DC3	DC3 Science Team (2013)	Airborne	2012	Salina, KS	13 May – 30 Jun
SOAS	SOAS Science Team (2013)	Ground	2013	Centreville, AL	1 Jun – 15 Jul
SEAC4RS	SEAC4RS Science Team (2014)	Airborne	2013	Houston, TX	8 Aug – 23 Sep
FRAPPÉ	FRAPPÉ Science Team (2014)	Airborne	2014	Broomfield, CO	16 Jul –16 Aug
KORUS-AQ	KORUS-AQ Science Team (2018)	Airborne	2016	Pyeongtaek, ROK	1 May – 14 Jun
				Palmdale, CA	17 Jun – 18 Jun

The fraction of total $\mathrm{NO_x}$ loss occurring via $\mathrm{RONO_2}$ chemistry from all 13 of these campaigns is shown in Fig. 3a for points within the continental summertime boundary layer. Despite spanning a large range of environments, all 13 campaigns are well described by a single function of the form $(1+b\cdot(\frac{\mathrm{NO2R}}{\mathrm{VOCR}})^{m})^{-1}$ (red line in Fig. 3a). This ~~roughly matches the expected form~~ functional form corresponds to a linear relationship between $P(\mathrm{RONO_2})/P(\mathrm{HNO_3})$ and NO2R/VOCR on a log-log scale. If m is fixed to 1, then this form also corresponds to the expected behavior if the VOC mixture ~~were constant~~ did not change between environments, and so all parameters other than NO2R/VOCR remained constant (gray line in Fig. 3a). ~~However, the observations exhibit a sharper transition from $\mathrm{HNO_3}$-dominated to $\mathrm{RONO_2}$-dominated $\mathrm{NO_x}$ loss, likely due to an increase in α_{eff} as NO2R/VOCR decreases.~~

The calculated increase in fractional $\mathrm{NO_x}$ loss via $\mathrm{RONO_2}$ chemistry as NO2R/VOCR decreases is matched by an increase in the observed ratio of $\Sigma\mathrm{RONO_2}$ to the sum of $\Sigma\mathrm{RONO_2}$ and $\mathrm{HNO_3}$ (Fig. 3b). However, the increase in fractional concentrations as NO2R/VOCR decreases is much less than the increase in fractional production. At low NO2R/VOCR ratios, the

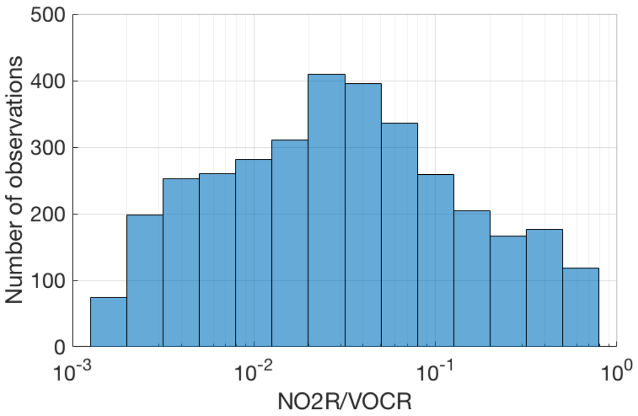

Figure 2. ~~Comparison~~ Number of ~~the relative production rates of $RONO_2$ and HNO_3 as a function of NO2R/VOCR. Used data~~ points ~~are restricted to~~ in each bin for which the ~~continental summertime boundary layer (i.e., over land, less than 1.5 km above ground level, and average temperature > 10 °C). The top panel shows the~~ fraction of NO_x loss ~~attributable to~~ occurring via $RONO_2$ chemistry ~~, as well as a least-squares fit to the data and the expected behavior if α_{eff}, $f_{NO_{\mathrm{eff}}}$, $Y_{RO_{2\mathrm{eff}}}$ were constant~~could be calculated. ~~The bottom panel shows the ratio of $\Sigma RONO_2$ to the sum of HNO_3 and $\Sigma RONO_2$. In each panel, the blue diamonds show the median in each bin and the vertical lines show the interquartile range.~~

dominant $RONO_2$ species are typically short lived and can undergo heterogeneous hydrolysis to produce HNO_3 (e.g., Browne et al., 2013). This indirect source of HNO_3 can be the greatest source of HNO_3 in forested environments, and leads to the relatively weak dependence of fractional concentration on NO2R/VOCR.

While the fraction of NO_x loss occurring via $RONO_2$ chemistry can be well predicted from just the NO2R/VOCR ratio, the observations exhibit a sharper transition from HNO_3-dominated to $RONO_2$-dominated NO_x loss than would be expected if the VOC mixture remained constant. This effect can be explained by variation in $Y_{RO_{2\mathrm{eff}}}$, α_{eff}, and $f_{NO_{\mathrm{eff}}}$ as NO2R/VOCR changes. The behavior of these three parameters is shown in Fig. 4. As NO2R/VOCR decreases, $f_{NO_{\mathrm{eff}}}$ consistently decreases from 0.8 to 0.2, due almost entirely to the decrease in NO_x concentrations. In contrast, both $Y_{RO_{2\mathrm{eff}}}$ and α_{eff} are larger in areas with low NO2R/VOCR ratios, due to changes in the VOC mixture between environments. In areas where NO2R/VOCR is high, many of the predominant VOCs, including CO, HCHO, and aromatics, either do not produce RO_2 radicals when oxidized by OH or produce RO_2 radicals that do not efficiently produce organic nitrates, leading to the relatively low values of both these parameters. In areas with low NO2R/VOCR ratios, the VOC mixture is often dominated by biogenic alkenes such as isoprene and monoterpenes that efficiently produce organic nitrates, leading to higher values of both $Y_{RO_{2\mathrm{eff}}}$ and α_{eff}. However, although variation in these parameters can help explain some of the observed behavior of fractional NO_x loss, the overall variation is much smaller than the variation of the NO2R/VOCR ratio. Each of the three parameters varies by a factor of 4 or less, while the NO2R/VOCR ratio varies by a factor of 1000.

The conclusion that variation in VOC parameters is small compared to the variation in the NO2R/VOCR ratio does not hold outside of the summertime continental boundary layer. In the remote marine boundary layer or in the upper troposphere, α_{eff}

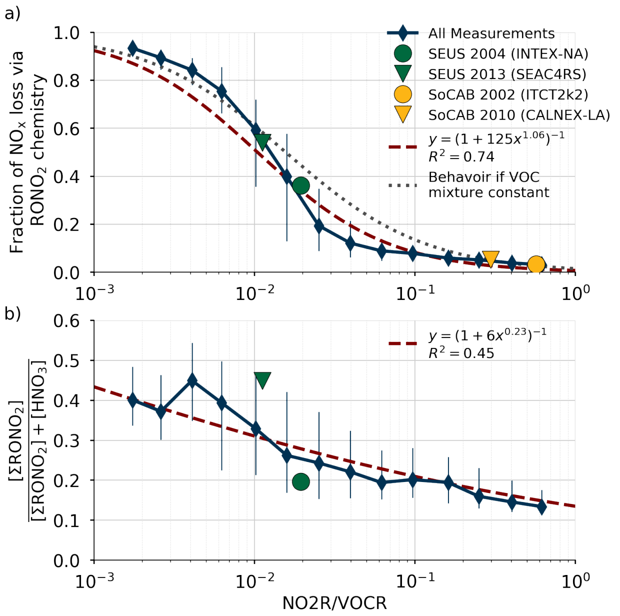

Figure 3. Comparison of the relative production rates of $RONO_2$ and HNO_3 as a function of NO2R/VOCR. Used data points are restricted to the continental summer daytime boundary layer (i.e., over land, less than 1.5 km above ground level, and average temperature > 10 °C). The top panel shows the fraction of NO_x loss attributable to $RONO_2$ chemistry, as well as a least-squares fit to the data and the expected behavior if α_{eff}, $f_{\mathrm{NO_{eff}}}$, $Y_{\mathrm{RO_{2}eff}}$ were constant. The bottom panel shows the ratio of $\Sigma RONO_2$ to the sum of HNO_3 and $\Sigma RONO_2$. In each panel, the blue diamonds show the median in each bin and the vertical lines show the interquartile range.

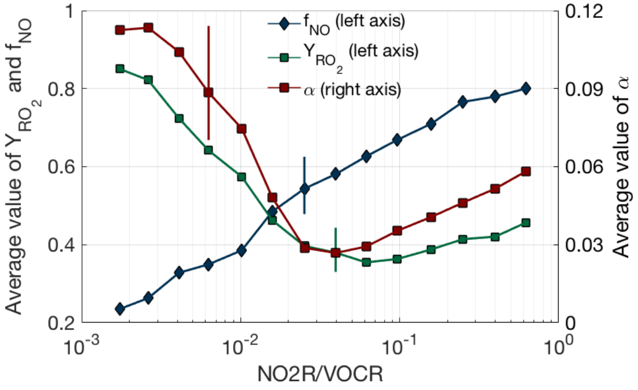

Figure 4. VOC oxidation parameters (α_{eff}, $f_{\mathrm{NO_{eff}}}$, $Y_{\mathrm{RO_{2}eff}}$) as a function of NO2R/VOCR. Used data points are restricted to the continental summer daytime boundary layer (i.e., over land, less than 1.5 km above ground level, and average temperature > 10 °C). The line and solid shapes show the median in each bin, and the vertical lines show an example of the interquartile range for each binned parameter.

is extremely low, as the dominant VOCs produce alkyl nitrates at yields of 0.01 or less (Mao et al., 2009; Perring et al., 2013). Under these conditions, HNO_3 dominates NO_x loss even when NO2R/VOCR is less than ~~3×10^{-1}~~3×10^{-2}.

The trend calculated from the in situ observations matches that found in model simulations, that in areas with high ratios of NO2R to VOCR, HNO_3 is the dominant NO_x sink, but as concentrations of NO_x decrease and concentrations of VOCs increase, the opposite is true. The combined in situ observations show that the importance of $RONO_2$ chemistry to NO_x loss is a non-linear function of the NO2R/VOCR ratio, leading to a sharp transition between the HNO_3-dominated and $RONO_2$-dominated regimes. The sharp transition suggests there is a strong gradient in chemical NO_x loss between urban and rural areas, especially in areas with significant biogenic VOC emissions. Furthermore, the sharp transition indicates that some regions may quickly shift from being HNO_3-dominated to $RONO_2$-dominated if NO2R/VOCR decreases.

3.2 Nighttime chemistry

While the primary focus of this analysis is on daytime chemistry, a conceptually similar transition may also occur at night. At night, OH concentrations are near zero, and the first step in NO_x oxidation is the reaction of NO_2 with O_3 to produce NO_3. This radical can in turn react either with NO_2 to form N_2O_5 or with an alkene to form an organic nitrate (R8 – R9).

$$NO_3 + RH \rightarrow RONO_2 \tag{R8}$$

$$NO_3 + NO_2 \rightleftharpoons N_2O_5 \tag{R9}$$

Finally, N_2O_5 can either thermally decompose to reform NO_3 and NO_2 or it can hydrolyze on aerosol surfaces to produce HNO_3 (R9 – R10).

$$N_2O_5 \xrightarrow{k_{\mathrm{hyd}}} 2\,HNO_3 \tag{R10}$$

Although the details of the nighttime chemical system are different, it shares some fundamental similarities with the daytime system: NO_x can be lost through the production of $RONO_2$ or of HNO_3, and a key step controlling the relative importance of these two sinks is whether an oxidant reacts with NO_2 or with a VOC. These similarities suggest that the relative importance of $RONO_2$ and HNO_3 as NO_x sinks at night may be controlled by the relative reactivities of NO_2 and VOCs towards NO_3. In areas where NO_3 is more likely to react with NO_2, HNO_3 production is likely to dominate NO_x loss, while the opposite is likely to be true in areas where NO_3 is more likely to react with a VOC.

However, quantitatively estimating the relative fraction of NO_x loss through these different pathways is not practical with the combined dataset presented here. There have been relatively few measurement of the nocturnal atmosphere (only 4 of the 13 campaigns in Table 1 include nighttime measurements) and there remain significant uncertainties in the kinetics of nighttime NO_x loss. In particular, the overall rate of N_2O_5 hydrolysis is controlled by the reactive uptake parameter γ and the aerosol surface area, both of which can vary by multiple orders of magnitude (McDuffie et al., 2018; Brown et al., 2009). Variation in the rate of N_2O_5 hydrolysis may therefore also play a major role in controlling the relative importance of $RONO_2$ and HNO_3

chemistry to NO_x loss at night. While developing a more quantitative understanding of the trends in the chemical mechanisms of nocturnal NO_x loss is an important area for future research, the conceptual similarity between the daytime and nighttime regimes suggests that conclusions based on daytime NO_x chemistry may also be relevant to the nighttime.

4 Predicted trends over time

Using the trends in Fig. 3a to understand trends in NO_x chemistry over time is only possible if the response to variation across space is equivalent to the response to variation across time. Two direct comparisons of fractional NO_x loss in the same environment but at different times are found to fall along the same curve as the variation between campaigns in different locations (Fig. 3), indicating that such a substitution is valid in this analysis. The first case, INTEX-NA and SEAC4RS, sampled the southeast United States (SEUS) in 2004 and 2013; the second case, ITCT2k2 and CALNEX-P3, sampled the South Coast Air Basin (SoCAB) around Los Angeles in 2002 and 2010. Averages from these pairs of campaigns are shown in Fig. 3a and all four points fall along the same overall curve. For INTEX-NA and SEAC4RS, the shift in chemistry towards the $RONO_2$-dominated regime is accompanied by a dramatic shift in the ratio of $\Sigma RONO_2$ and HNO_3 concentrations, where $\Sigma RONO_2$ concentrations were only one quarter of HNO_3 in 2004 but were nearly equal to HNO_3 in 2013. $\Sigma RONO_2$ measurements are not available for ITCT2k2 or CALNEX-P3, preventing a similar comparison from being made for those campaigns.

Together, these cases indicate that the trend from Fig. 3a can be used to predict changes in fractional loss if the trend in $NO2R/VOCR$ is known. Over the past decade, satellite measurements of NO_2 show a significant decrease in national NO_2 concentrations, reporting an average decrease of 4.5–7 % per year between 2005 and 2011 (Russell et al., 2012). No comparable satellite observations of VOCs exist, but studies in multiple locations have reported a decrease in primary anthropogenic VOC concentrations of 5.5–7.5 % per year over 2000-2010 (Geddes et al., 2009; Warneke et al., 2012; Pollack et al., 2013; Pusede et al., 2014). In contrast, biogenic VOC concentrations have been either constant or increasing over that same time period (Geddes et al., 2009; Hidy et al., 2014). Oxygenated VOCs show no major trend with time, although there are few long-term measurements of these species (Geddes et al., 2009; Pusede et al., 2014).

These varied trends in NO_x, anthropogenic VOCs, and biogenic VOCs mean that $NO2R/VOCR$ has not changed uniformly over the past decade. Past $NO2R/VOCR$ ratios were calculated by assuming a 6.5% yr^{-1} decrease to anthropogenic VOC concentrations, a 5.5% yr^{-1} decrease to NO_x concentrations, and a 1.5% yr^{-1} increase in biogenic VOC concentrations over the past 15 years. We also extrapolate these same trends to estimate $NO2R/VOCR$ 15 years into the future. The calculated $NO2R/VOCR$ ratios are combined with the relationship from Fig. 3 to estimate fractional NO_x loss at different times (Fig. 5). Based on these trends, $RONO_2$ chemistry is seen to have become a larger portion of total NO_x loss over the past 15 years, although the change is not evenly distributed. The similar trends in NO_x and anthropogenic VOCs cause there to have been little to no change in the regions with the highest $NO2R/VOCR$ ratios (typically large cities). The largest changes are projected to occur in regions with moderate $NO2R/VOCR$ ratios. In these regions, biogenic VOCs often account for a greater fraction of the VOCR, leading to significant decreases in $NO2R/VOCR$ over the past 15 years. In addition, the response of fractional loss to changes in the $NO2R/VOCR$ ratio is magnified in areas where both $RONO_2$ and HNO_3 chemistry contribute to NO_x

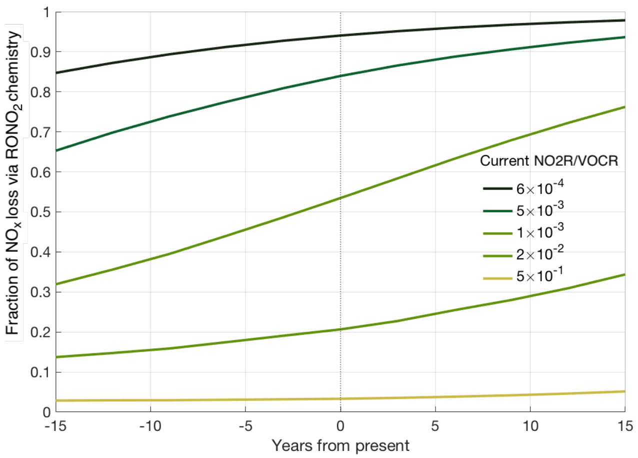

Figure 5. Predicted trends in fractional NO$_x$ loss over time, calculated from the estimated NO2R/VOCR ratio assuming a constant -6.5% yr^{-1} decrease in anthropogenic VOC concentrations, a 5.5% yr^{-1} decrease in NO$_x$ concentrations, and a 1.5% yr^{-1} increase in biogenic VOC concentrations.

loss. In this transitional regime, if recent trends continue, the fraction of NO$_x$ loss occurring via RONO$_2$ chemistry could double in the next 15 years. ~~Many~~ Given the large number of data points sampled in this transition regime (Fig. 2), many regions of the United States are therefore likely to transition from a regime where HNO$_3$ dominates NO$_x$ loss to a mixed or RONO$_2$-dominated regime.

5 Impacts of the transition from the HNO$_3$ to the RONO$_2$ regime

The growing importance of RONO$_2$ chemistry to NO$_x$ loss has several implications for air quality. Most directly, it means that understanding NO$_x$ chemistry in all but the most polluted megacities requires including the effects of RONO$_2$ chemistry. More theoretically, the transition from HNO$_3$- to RONO$_2$-dominated NO$_x$ loss affects how atmospheric chemistry will respond to changes in emissions of NO$_x$ and VOCs. Because RONO$_2$ are produced in the same set of reactions that produce O$_3$, the fractional loss of NO$_x$ via RONO$_2$ chemistry is directly proportional to the ozone production efficiency (OPE), the ratio of ozone production to NO$_x$ loss (Eq. 5).

$$\mathrm{OPE} = \frac{P(\mathrm{O3})}{L(\mathrm{NO_x})}\,\frac{P(\mathrm{O_3})}{L(\mathrm{NO_x})} = \frac{2\cdot \mathrm{VOCR}\cdot Y_{\mathrm{RO_2}_{\mathrm{eff}}}\cdot f_{\mathrm{NO}_{\mathrm{eff}}}\cdot(1-\alpha_{\mathrm{eff}})}{\mathrm{NO2R}+\mathrm{VOCR}\cdot Y_{\mathrm{RO_2}_{\mathrm{eff}}}\cdot f_{\mathrm{NO}_{\mathrm{eff}}}\cdot \alpha_{\mathrm{eff}}} \propto \frac{P(\mathrm{RONO_2})}{P(\mathrm{RONO_2})+P(\mathrm{HNO_3})} \tag{5}$$

Fundamentally, OPE represents the total amount of ozone produced for each molecule of NO$_x$ emitted. When considering ozone pollution on regional scales, OPE is a more ~~comprehensive~~ appropriate metric than instantaneous ozone production because it accounts for ozone production both locally and further afield.

Figure 6 uses the theoretic framework described in Romer et al. (2018) to investigate how ozone and NO$_x$ chemistry change as a function of NO2R/VOCR. As the NO2R/VOCR ratio decreases, OPE increases, reaching an inflection point exactly at

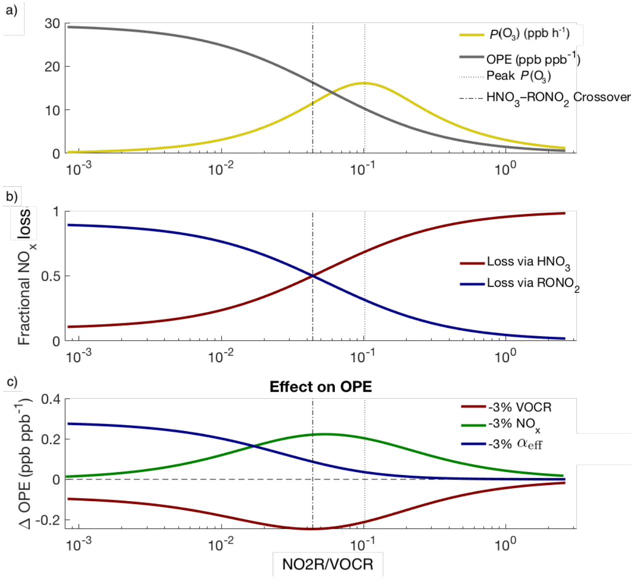

Figure 6. Theoretical picture of $\mathrm{NO_x}$ and $\mathrm{O_3}$ chemistry, calculated using variable $\mathrm{NO_x}$ concentrations and fixed VOCR, $P(\mathrm{HO_x})$, and α_{eff}. Panel a shows how $P(\mathrm{O_3})$ and OPE change as $\mathrm{NO_x}$ changes; Panel b shows how the fractional $\mathrm{NO_x}$ loss changes as NO2R/VOCR decreases; Panel c shows that changes to $\mathrm{NO_x}$ and VOCR have their greatest effect on OPE not when PO_3 is at a maximum, but at the crossover point between the $\mathrm{RONO_2}$-dominated and $\mathrm{HNO_3}$-dominated regimes.

the crossover point between the $\mathrm{HNO_3}$-dominated and $\mathrm{RONO_2}$-dominated regimes (Fig. 6a–b). For the polluted areas in the country, where $\mathrm{HNO_3}$ is currently the dominant $\mathrm{NO_x}$ loss pathway, this means that, for example, interventions to improve air quality by reducing $\mathrm{NO_x}$ emissions will be fighting uphill, because every incremental fractional decrease in $\mathrm{NO_x}$ emissions will be associated with a growing incremental increase in OPE (Fig. 6c).

In addition, as $\mathrm{RONO_2}$ chemistry becomes a more important part of the $\mathrm{NO_x}$ budget, changes to α_{eff} have an increasing effect on OPE (Fig. 6c). Policy interventions that reduce VOCR but preferentially target high-α compounds (e.g., long-chain alkanes) could inadvertently increase ozone production or OPE (Farmer et al., 2011; Perring et al., 2013).

In addition to the large effects on aerosol yield that changes to $\mathrm{NO_x}$ and VOC emissions have directly (e.g., Xu et al., 2015a; Pusede et al., 2016), they also affect aerosols by changing the fate of $\mathrm{NO_x}$. While both $\mathrm{HNO_3}$ and $\mathrm{RONO_2}$ can form aerosols (Stelson and Seinfeld, 1982; Pye et al., 2015), the properties of the resulting aerosols are likely to differ. Because $\mathrm{HNO_3}$ is a strong acid, a shift towards $\mathrm{RONO_2}$ chemistry is likely to increase aerosol pH. An increase in the role of $\mathrm{RONO_2}$ chemistry will also cause more of the nitrate aerosol to be organic rather than inorganic, potentially affecting the viscosity and morphology of aerosols.

Further effects of changing $\mathrm{NO_x}$ chemistry arise from the distinct fates of $\mathrm{RONO_2}$ and $\mathrm{HNO_3}$. Many $\mathrm{RONO_2}$ compounds, especially those derived from isoprene, are remarkably reactive in the troposphere, with lifetimes of a few hours or less. A fraction of this $\mathrm{RONO_2}$ loss returns $\mathrm{NO_x}$ to the atmosphere, allowing $\mathrm{RONO_2}$ production to effectively transport $\mathrm{NO_x}$

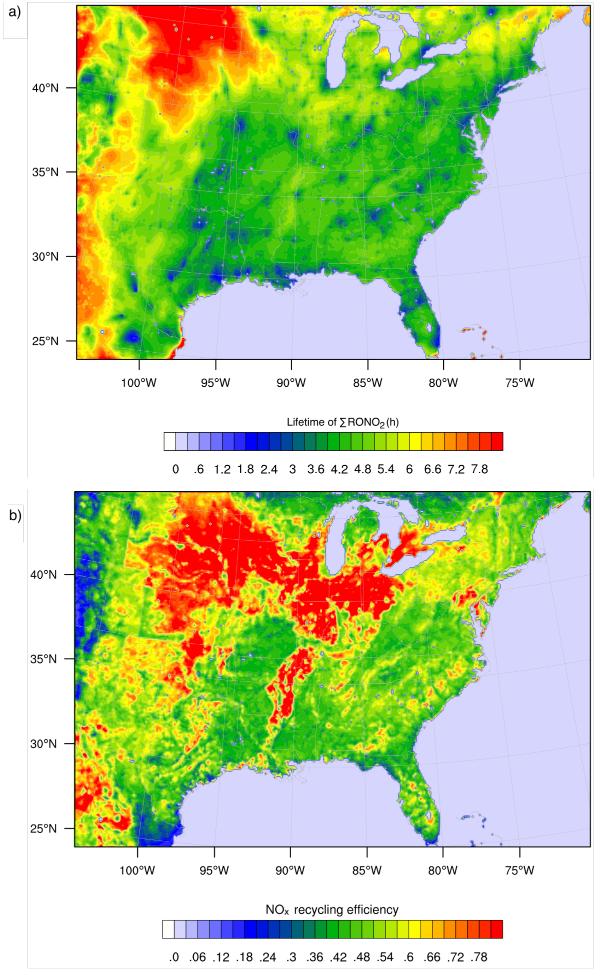

Figure 7. WRF-Chem simulation of $RONO_2$ chemistry over the southeast United States for summer 2013 as described in Zare et al. (2018). Panel a shows the overall lifetime of $\Sigma RONO_2$, defined as the concentration of $\Sigma RONO_2$ divided by their chemical loss rate for the daytime boundary layer. Panel b shows the average NO_x recycling efficiency, defined as the local rate of NO_x production from $RONO_2$ oxidation divided by the rate of $RONO_2$ production.

downwind (Romer et al., 2016; Xiong et al., 2016). In contrast, HNO_3 is effectively chemically inert in the troposphere, with a chemical lifetime of 50 hours or more.

As a result of the differing chemical fates and lifetimes, transitioning from a HNO_3-dominated regime to a mixed or $RONO_2$-dominated regime has implications for the distribution of NO_x on regional to continental scales. If a greater fraction of NO_x in polluted or moderately polluted regions is converted into $RONO_2$ compounds rather than into HNO_3, then more of the NO_x may be re-released downwind, where it can participate in radical chemistry and ozone production. Simulations of $RONO_2$ chemistry using WRF-Chem and the RACM2_Berkeley2 mechanism (Zare et al., 2018) were used to investigate the

$RONO_2$ lifetime and NO_x recycling efficiency of $RONO_2$ across the southeast United States in summer 2013 (Fig. 7). Across much of the region, $\Sigma RONO_2$ are calculated to have a lifetime of roughly 4 hours, and the release of NO_x from $RONO_2$ oxidation was between 40 and 75% of the instantaneous $RONO_2$ production rate. Combined, these findings demonstrate a significant role for $RONO_2$ chemistry in the transport of NO_x between regions in the southeast United States. The effects of organic nitrate chemistry on the distribution of NO_x is likely to vary greatly across different regions of the United States and should be studied in further detail.

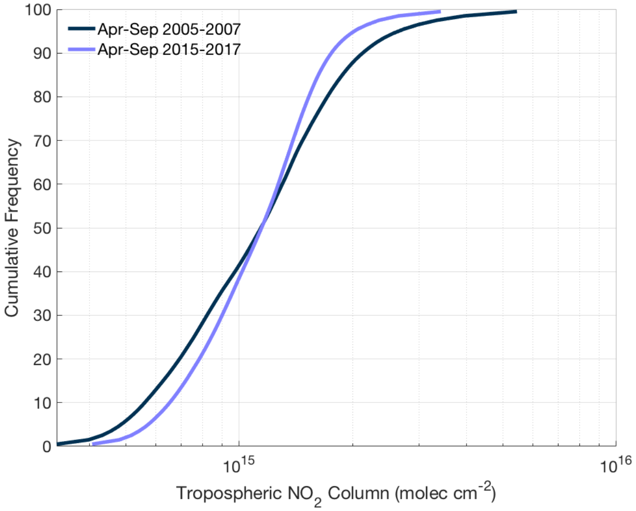

Figure 8. Cumulative frequency distribution of OMI tropospheric NO_2 columns over the continental United States using the BEHR v3.0A retrieval for summer (Apr–Sep) in 2005–2007 and 2015–2017.

Enhanced NO_x transport between source and receptor regions is one aspect of a combined trend that is transforming the spatial distribution of NO_x. Over the past decade, NO_x emission reductions have been concentrated in the most polluted environments. In these areas, motor vehicles and power plants, targets of emission control strategies, account for almost all of the NO_x emissions. In less polluted regions, other sources of NO_x, including soil microbes (both in agricultural and non-agricultural regions), off-road vehicles, fires, and lightning, play a greater role in the NO_x budget, reducing the effectiveness of typical combustion-related NO_x emission controls. In addition, hemispheric background concentrations of NO_x and O_3 have risen slightly over the past two decades (Cooper et al., 2012). The combination of all three of these trends suggests that the distribution of NO_x across the United States is getting flatter over time. This trend matches satellite observations of NO_2 over the continental United States. Figure 8 shows the cumulative frequency distribution of summertime tropospheric NO_2 columns from 2005-2007 and 2015-2017 using the BErkeley High-Resolution (BEHR) v3.0A retrieval (Laughner et al., 2018) of slant-column measurements from OMI. Over this time, the highest percentiles NO_2 concentrations have decreased and the lowest percentiles increased, leading to a significantly narrower distribution of NO_2 concentrations.

In summary, over the past 15 years, decreases in anthropogenic NO_x and VOC emissions have led to a significant shift in the mechanisms of daytime NO_x loss. Many places where HNO_3 production dominated NO_x loss are now mixed or have switched to a situation where the majority of NO_x loss occurs through $RONO_2$ chemistry. If past trends continue, $RONO_2$ chemistry will grow to become an even more important fraction of NO_x chemistry in coming decades. As a result of this combination of changing NO_x chemistry, decreasing NO_x emissions, and increasing background concentrations, air pollution in the United States may transform from a highly local issue to a more extended regional one. Efforts to control air pollution focused only on local sources are less likely to be effective; future improvements in air quality and attaining the most recent National Ambient Air Quality Standards are likely to require coordinated efforts on regional scales to broadly reduce NO_x emissions.

Data availability. Data from ARCTAS, DC3, FRAPPÉ, INTEX-NA, INTEX-B, KORUS-AQ and SEAC4RS are available from https://www-air.larc.nasa.gov/missions.htm. Data from ITCT2k2, CALNEX, SOAS, UBWOS, and WINTER are available from https://www.esrl.noaa.gov/csd/field.html. The BEHR retrieval of OMI NO_2 columns is available at http://behr.cchem.berkeley.edu/.

Appendix A: Calculation of the $RONO_2$ production rate

A1 Steady-state calculation of unmeasured radicals

The formation rates of $RONO_2$, HNO_3, and O_3 depend either directly or indirectly on the concentration of OH, HO_2, RO_2, NO, and NO_2. Speciated RO_2 radicals are not currently observable in the atmosphere, and thus all RO_2 concentrations were calculated assuming they were in steady-state, with their production and loss rates equal.

There were additional periods in which some combination of OH, HO_2, and NO were also not measured, and these radicals were also assumed to be in steady state. Concentrations of VOCs, NO_2, and O_3 were always taken from measurements. In order to calculate the steady-state concentrations of unmeasured radicals, reaction rate constants and RO_2 yields for the different VOCs were taken from the MCM v3.3.1 (Jenkin et al., 2015). Concentrations of all unmeasured species were calculated iteratively until all the concentrations converged. Equations (A1–~~A7~~A8) were used to calculate the steady-state concentration of unmeasured radicals.

$$\begin{aligned}
P(\mathrm{RO_2}) &= [\mathrm{OH}]\cdot\mathrm{VOCR}\cdot Y_{\mathrm{RO_2}}\\
L(\mathrm{RO_2}) &= k_{\mathrm{RO_2+NO}}[\mathrm{RO_2}][\mathrm{NO}] + k_{\mathrm{RO_2+HO_2}}[\mathrm{RO_2}][\mathrm{HO_2}] + 2k_{\mathrm{RO_2+RO_2}}[\mathrm{RO_2}][\mathrm{RO_2}] + k_{\mathrm{isom}}\\
P(\mathrm{HO_2}) &= k_{\mathrm{RO_2+NO}}[\mathrm{RO_2}][\mathrm{NO}](1-\alpha) + [\mathrm{OH}]\cdot\mathrm{VOCR}\cdot Y_{\mathrm{HO_2}} + 2j_{\mathrm{HCHO}}\\
L(\mathrm{HO_2}) &= k_{\mathrm{HO_2+NO}}[\mathrm{HO_2}][\mathrm{NO}] + 2k_{\mathrm{HO_2+HO_2}}[\mathrm{HO_2}][\mathrm{HO_2}] + k_{\mathrm{HO_2+RO_2}}[\mathrm{HO_2}][\mathrm{RO_2}]\\
P(\mathrm{NO}) &= j_{\mathrm{NO_2}}[\mathrm{NO_2}]\\
L(\mathrm{NO}) &= k_{\mathrm{O_3+NO}}[\mathrm{O_3}][\mathrm{NO}] + k_{\mathrm{RO_2+NO}}[\mathrm{RO_2}][\mathrm{NO}] + k_{\mathrm{HO_2+NO}}[\mathrm{HO_2}][\mathrm{NO}]\\
P(\mathrm{OH}) &= \frac{2j_{\mathrm{O_3\to O^1D}}[\mathrm{O_3}]k_{\mathrm{O^1D+H_2O}}}{k_{\mathrm{O^1D+H_2O}}[\mathrm{H_2O}] + k_{\mathrm{O^1D+O_2}}[\mathrm{O_2}] + k_{\mathrm{O^1D+N_2}}[\mathrm{N_2}]} + k_{\mathrm{HO_2+NO}}[\mathrm{HO_2}][\mathrm{NO}]\\
L(\mathrm{OH}) &= \mathrm{VOCR} + \mathrm{NO2R}
\end{aligned}$$

In (A8), the symbol XR is used to represent the OH reactivity of species such as SO_2 and O_3 that are not included in either VOCR or NO2R. Although it is not often categorized as a VOC, CO is included as a contributor to VOCR. The reaction rate constant for NO_2 with OH was taken from Mollner et al. (2010), with temperature- and pressure-dependencies from Henderson et al. (2012).

$$P(\mathrm{RO_2}) = [\mathrm{OH}]\cdot\mathrm{VOCR}\cdot Y_{\mathrm{RO_2}} \tag{A1}$$

$$L(\mathrm{RO_2}) = k_{\mathrm{RO_2+NO}}[\mathrm{RO_2}][\mathrm{NO}] + k_{\mathrm{RO_2+HO_2}}[\mathrm{RO_2}][\mathrm{HO_2}] + 2k_{\mathrm{RO_2+RO_2}}[\mathrm{RO_2}][\mathrm{RO_2}] + k_{\mathrm{isom}}[\mathrm{RO_2}] \tag{A2}$$

$$P(\mathrm{HO_2}) = k_{\mathrm{RO_2+NO}}[\mathrm{RO_2}][\mathrm{NO}](1-\alpha) + [\mathrm{OH}]\cdot\mathrm{VOCR}\cdot Y_{\mathrm{HO_2}} + 2j_{\mathrm{HCHO}}[\mathrm{HCHO}] \tag{A3}$$

$$L(\mathrm{HO_2}) = k_{\mathrm{HO_2+NO}}[\mathrm{HO_2}][\mathrm{NO}] + 2k_{\mathrm{HO_2+HO_2}}[\mathrm{HO_2}][\mathrm{HO_2}] + k_{\mathrm{HO_2+RO_2}}[\mathrm{HO_2}][\mathrm{RO_2}] \tag{A4}$$

$$P(\mathrm{NO}) = j_{\mathrm{NO_2}}[\mathrm{NO_2}] \tag{A5}$$

$$L(\mathrm{NO}) = k_{\mathrm{O_3+NO}}[\mathrm{O_3}][\mathrm{NO}] + k_{\mathrm{RO_2+NO}}[\mathrm{RO_2}][\mathrm{NO}] + k_{\mathrm{HO_2+NO}}[\mathrm{HO_2}][\mathrm{NO}] \tag{A6}$$

$$P(\mathrm{OH}) = \frac{2j_{\mathrm{O_3\to O^1D}}[\mathrm{O_3}]\cdot k_{\mathrm{O^1D+H_2O}}[\mathrm{H_2O}]}{k_{\mathrm{O^1D+H_2O}}[\mathrm{H_2O}] + k_{\mathrm{O^1D}+M}[M]} + j_{\mathrm{HONO}}[\mathrm{HONO}] + k_{\mathrm{HO_2+NO}}[\mathrm{HO_2}][\mathrm{NO}] + k_{\mathrm{O_3+RH}}[\mathrm{O_3}][\mathrm{RH}]Y_{\mathrm{OH}} \tag{A7}$$

$$L(\mathrm{OH}) = (\mathrm{VOCR} + \mathrm{NO2R} + \mathrm{XR})[\mathrm{OH}] \tag{A8}$$

In order to test the accuracy of the modeling, we used periods when HO_2, OH, and NO were all measured and calculated how the production ratio $P(\mathrm{RONO_2})/P(\mathrm{HNO_3})$ changed if modeled radical concentrations were used instead. These results are shown in Fig. A1. Even in the worst-case scenario (modeled concentrations used for all radicals), the slope is close to one (Fig. A1a), indicating that the use of modeled radicals does not significantly affect our results. Furthermore, Fig. A1b–d show that the use of modeled OH or HO_2 concentrations alone does not lead to noticeable changes in $P(\mathrm{RONO_2})/P(\mathrm{HNO_3})$. Use of modeled NO concentrations can cause small but noticeable changes in $P(\mathrm{RONO_2})/P(\mathrm{HNO_3})$, but modeled NO concentrations are used in less than 3% of all data points used in this analysis (238 out of 7988 data points).

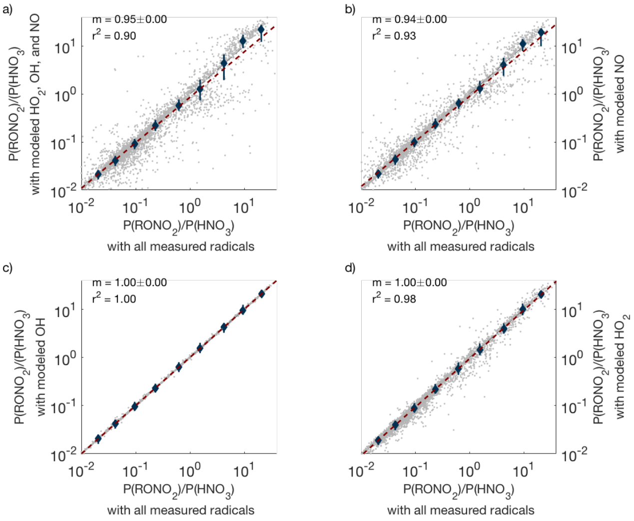

Figure A1. Comparison of $P(\mathrm{RONO_2})/P(\mathrm{HNO_3})$ when measured concentrations of all possible radicals are used (x-axis) versus when measured concentrations are replaced by modeled concentrations (y-axis). Panel a shows the result when modeled concentrations of OH, $\mathrm{HO_2}$, and NO are all used simultaneously; Panels b–d show the effect of replacing measured with modeled values one species at a time.

A2 Determination of α

Accurately calculating the $\mathrm{RONO_2}$ production rate requires accurate knowledge of α_i for all VOCs. If values of α had been reported for a specific compound from laboratory measurements, the most recent value was applied (Perring et al., 2013; Teng et al., 2015; Rindelaub et al., 2015; Praske et al., 2015; Wennberg et al., 2018). In cases where no reliable laboratory measurements are available, the parameterization for α from Wennberg et al. (2018) was used. In all cases, the temperature- and pressure-dependencies described in Wennberg et al. (2018) were used to scale the laboratory measurements of α to the conditions of the atmosphere.

Author contributions. PSRP and RCC designed the experiment, PSRP performed the analysis of field campaign data and wrote the paper with contributions from all authors, AZ designed, ran, and analyzed the modeling simulations. RCC supervised the project

Competing interests. The authors declare that they have no conflict of interest.

Acknowledgements. This study was supported by NOAA grant NA18OAR4310117 in the Atmospheric Chemistry, Carbon Cycle, and Climate program of the NOAA Climate Program Office and by NSF grant AGS-1352972. The authors thank Josh Laughner for assistance with the OMI BEHR retrieval.

References

ARCTAS-B Science Team: ARCTAS-B DC-8 aircraft data, NASA, https://www-air.larc.nasa.gov/cgi-bin/ArcView/arctas, 2011.

BEAPREX 07 Science Team: BEARPEX 2007 field campaign data, 2007.

BEAPREX 09 Science Team: BEARPEX 2009 field campaign data, 2009.

Brown, S. S., Dubé, W. P., Fuchs, H., Ryerson, T. B., Wollny, A. G., Brock, C. A., Bahreini, R., Middlebrook, A. M., Neuman, J. A., Atlas, E., Roberts, J. M., Osthoff, H. D., Trainer, M., Fehsenfeld, F. C., and Ravishankara, A. R.: Reactive uptake coefficients for N_2O_5 determined from aircraft measurements during the Second Texas Air Quality Study: Comparison to current model parameterizations, J. Geophys. Res., 114, D00F10, https://doi.org/10.1029/2008JD011679, 2009.

Browne, E. C. and Cohen, R. C.: Effects of biogenic nitrate chemistry on the NO_x lifetime in remote continental regions, Atmos. Chem. Phys., 12, 11 917–11 932, https://doi.org/10.5194/acp-12-11917-2012, 2012.

Browne, E. C., Min, K.-E., Wooldridge, P. J., Apel, E., Blake, D. R., Brune, W. H., Cantrell, C. A., Cubison, M. J., Diskin, G. S., Jimenez, J. L., Weinheimer, A. J., Wennberg, P. O., Wisthaler, A., and Cohen, R. C.: Observations of total $RONO_2$ over the boreal forest: NO_x sinks and HNO_3 sources, Atmos. Chem. Phys., 13, 4543–4562, https://doi.org/10.5194/acp-13-4543-2013, http://www.atmos-chem-phys.net/13/4543/2013/acp-13-4543-2013.html, 2013.

CALNEX Science Team: CALNEX 2010 WP-3D data, NOAA, https://esrl.noaa.gov/csd/groups/csd7/measurements/2010calnex/P3/DataDownload/, 2002a.

CALNEX Science Team: CALNEX 2010 Bakersfield site data, NOAA, https://esrl.noaa.gov/csd/groups/csd7/measurements/2010calnex/Bakersfield/DataDownload/, 2002b.

Cooper, O. R., Gao, R.-S., Tarasick, D., Leblanc, T., and Sweeney, C.: Long-term ozone trends at rural ozone monitoring sites across the United States, 1990–2010, J. Geophys. Res. Atmos., 117, D22 307, https://doi.org/10.1029/2012JD018261, 2012.

DC3 Science Team: DC3 Field Campaign Data from DC-8 aircraft, NASA, https://doi.org/10.5067/aircraft/dc3/dc8/aerosol-tracegas, 2013.

Edwards, P. M., Young, C. J., Aikin, K., de Gouw, J., Dubé, W. P., Geiger, F., Gilman, J., Helmig, D., Holloway, J. S., Kercher, J., Lerner, B., Martin, R., McLaren, R., Parrish, D. D., Peischl, J., Roberts, J. M., Ryerson, T. B., Thornton, J., Warneke, C., Williams, E. J., and Brown, S. S.: Ozone photochemistry in an oil and natural gas extraction region during winter: simulations of a snow-free season in the Uintah Basin, Utah, Atmos. Chem. Phys., 13, 8955–8971, https://doi.org/10.5194/acp-13-8955-2013, 2013.

Farmer, D. K., Perring, A. E., Wooldridge, P. J., Blake, D. R., Baker, A., Meinardi, S., Huey, L. G., Tanner, D., Vargas, O., and Cohen, R. C.: Impact of organic nitrates on urban ozone production, Atmos. Chem. Phys., 11, 4085–4094, https://doi.org/10.5194/acp-11-4085-2011, 2011.

Fisher, J. A., Jacob, D. J., Travis, K. R., Kim, P. S., Marais, E. A., Chan Miller, C., Yu, K., Zhu, L., Yantosca, R. M., Sulprizio, M. P., Mao, J., Wennberg, P. O., Crounse, J. D., Teng, A. P., Nguyen, T. B., St. Clair, J. M., Cohen, R. C., Romer, P., Nault, B. A., Wooldridge, P. J., Jimenez, J. L., Campuzano-Jost, P., Day, D. A., Hu, W., Shepson, P. B., Xiong, F., Blake, D. R., Goldstein, A. H., Misztal, P. K., Hanisco, T. F., Wolfe, G. M., Ryerson, T. B., Wisthaler, A., and Mikoviny, T.: Organic nitrate chemistry and its implications for nitrogen budgets in an isoprene- and monoterpene-rich atmosphere: constraints from aircraft ($SEAC^4RS$) and ground-based (SOAS) observations in the Southeast US, Atmos. Chem. Phys., 16, 5969–5991, https://doi.org/10.5194/acp-16-5969-2016, http://www.atmos-chem-phys.net/16/5969/2016/, 2016.

Fowler, D., Coyle, M., Skiba, U., Sutton, M. A., Cape, J. N., Reis, S., Sheppard, L. J., Jenkins, A., Grizzetti, B., Galloway, J. N., Vitousek, P., Leach, A., Bouwman, A. F., Butterbach-Bahl, K., Dentener, F., Stevenson, D., Amann, M., and Voss, M.: The global nitrogen cycle in the twenty-first century, Philos. T. Roy. Soc. B, 368, https://doi.org/10.1098/rstb.2013.0164, 2013.

FRAPPÉ Science Team: FRAPPÉ C-130 aircraft data, NASA, https://www-air.larc.nasa.gov/cgi-bin/ArcView/discover-aq.co-2014?C130=1, 2014.

Geddes, J. A., Murphy, J. G., and Wang, D. K.: Long term changes in nitrogen oxides and volatile organic compounds in Toronto and the challenges facing local ozone control, Atmos. Environ., 43, 3407–3415, https://doi.org/10.1016/j.atmosenv.2009.03.053, http://www.sciencedirect.com/science/article/pii/S1352231009002507, 2009.

Henderson, B. H., Pinder, R. W., Crooks, J., Cohen, R. C., Carlton, A. G., Pye, H. O. T., and Vizuete, W.: Combining Bayesian methods and aircraft observations to constrain the HO$^{\cdot}$ + NO$_2$ reaction rate, Atmos. Chem. Phys., 12, 653–667, https://doi.org/10.5194/acp-12-653-2012, http://www.atmos-chem-phys.net/12/653/2012/acp-12-653-2012.html, 2012.

Hidy, G. M., Blanchard, C. L., Baumann, K., Edgerton, E., Tanenbaum, S., Shaw, S., Knipping, E., Tombach, I., Jansen, J., and Walters, J.: Chemical climatology of the southeastern United States, 1999–2013, Atmos. Chem. Phys., 14, 11 893–11 914, https://doi.org/10.5194/acp-14-11893-2014, 2014.

INTEX-A Science Team: INTEX-A DC-8 Aircraft data, NASA, https://doi.org/10.5067/asdcdaac/intexa/0008, 2006.

INTEX-B Science Team: INTEX-B DC-8 aircraft data, NASA, https://doi.org/10.5067/asdcdaac/intexb/0008, 2011.

ITCT Science Team: ITCT 2002 WP-3D Data, NOAA, https://esrl.noaa.gov/csd/groups/csd7/measurements/2002ITCT/P3/DataDownload/, 2002.

Jenkin, M. E., Young, J. C., and Rickard, A. R.: The MCM v3.3.1 degradation scheme for isoprene, Atmos. Chem. Phys., 15, 11 433–11 459, https://doi.org/10.5194/acp-15-11433-2015, http://www.atmos-chem-phys.net/15/11433/2015/, 2015.

KORUS-AQ Science Team: KorUS-AQ Airborne Mission, NASA, https://doi.org/10.5067/Suborbital/KORUSAQ/DATA01, 2018.

Laughner, J. L., Zhu, Q., and Cohen, R. C.: The Berkeley High Resolution Tropospheric NO$_2$ product, Earth Syst. Sci. Data, 10, 2069–2095, https://doi.org/10.5194/essd-10-2069-2018, 2018.

Lee, B. H., Mohr, C., Lopez-Hilfiker, F. D., Lutz, A., Hallquist, M., Lee, L., Romer, P., Cohen, R. C., Iyer, S., Kurtén, T., Hu, W., Day, D. A., Campuzano-Jost, P., Jimenez, J. L., Xu, L., Ng, N. L., Guo, H., Weber, R. J., Wild, R. J., Brown, S. S., Koss, A., de Gouw, J., Olson, K., Goldstein, A. H., Seco, R., Kim, S., McAvey, K., Shepson, P. B., Starn, T., Baumann, K., Edgerton, E. S., Liu, J., Shilling, J. E., Miller, D. O., Brune, W., Schobesberger, S., D'Ambro, E. L., and Thornton, J. A.: Highly functionalized organic nitrates in the southeast United States: Contribution to secondary organic aerosol and reactive nitrogen budgets, Proc. Natl. Acad. Sci. USA, 113, 1516–1521, https://doi.org/10.1073/pnas.1508108113, 2016.

Lee, L., Wooldridge, P. J., Gilman, J. B., Warneke, C., de Gouw, J., and Cohen, R. C.: Low temperatures enhance organic nitrate formation: evidence from observations in the 2012 Uintah Basin Winter Ozone Study, Atmos. Chem. Phys., 14, 12 441–12 454, https://doi.org/10.5194/acp-14-12441-2014, 2014.

Mao, J., Ren, X., Brune, W. H., Olson, J. R., Crawford, J. H., Fried, A., Huey, L. G., Cohen, R. C., Heikes, B., Singh, H. B., Blake, D. R., Sachse, G. W., Diskin, G. S., Hall, S. R., and Shetter, R. E.: Airborne measurement of OH reactivity during INTEX-B, Atmos. Chem. Phys., 9, 163–173, https://doi.org/10.5194/acp-9-163-2009, 2009.

McDuffie, E. E., Fibiger, D. L., Dubé, W. P., Lopez-Hilfiker, F., Lee, B. H., Thornton, J. A., Shah, V., Jaeglé, L., Guo, H., Weber, R. J., Reeves, J. M., Weinheimer, A. J., Schroder, J. C., Campuzano-Jost, P., Jimenez, J. L., Dibb, J. E., Veres, P., Ebben, C., Sparks, T. L., Wooldridge, P. J., Cohen, R. C., Hornbrook, R. S., Apel, E. C., Campos, T., Hall, S. R., Ullmann, K., and Brown, S. S.: Heterogeneous

N_2O_5 Uptake During Winter: Aircraft Measurements During the 2015 WINTER Campaign and Critical Evaluation of Current Parameterizations, J. Geophys. Res. Atmos., 123, 4345–4372, https://doi.org/10.1002/2018JD028336, https://agupubs.onlinelibrary.wiley.com/doi/abs/10.1002/2018JD028336, 2018.

Mollner, A. K., Valluvadasan, S., Feng, L., Sprague, M. K., Okumura, M., Milligan, D. B., Bloss, W. J., Sander, S. P., Martien, P. T., Harley, R. A., McCoy, A. B., and Carter, W. P. L.: Rate of Gas Phase Association of Hydroxyl Radical and Nitrogen Dioxide, Science, 330, 646–649, https://doi.org/10.1126/science.1193030, 2010.

Nguyen, T. B., Crounse, J. D., Teng, A. P., St. Clair, J. M., Paulot, F., Wolfe, G. M., and Wennberg, P. O.: Rapid deposition of oxidized biogenic compounds to a temperate forest, Proc. Natl. Acad. Sci. USA, 112, E392–E401, https://doi.org/10.1073/pnas.1418702112, http://www.pnas.org/content/112/5/E392, 2015.

Perring, A. E., Bertram, T. H., Farmer, D. K., Wooldridge, P. J., Dibb, J., Blake, N. J., Blake, D. R., Singh, H. B., Fuelberg, H., Diskin, G., Sachse, G., and Cohen, R. C.: The production and persistence of $\Sigma RONO_2$ in the Mexico City plume, Atmos. Chem. Phys., 10, 7215–7229, https://doi.org/10.5194/acp-10-7215-2010, http://www.atmos-chem-phys.net/10/7215/2010/, 2010.

Perring, A. E., Pusede, S. E., and Cohen, R. C.: An Observational Perspective on the Atmospheric Impacts of Alkyl and Multifunctional Nitrates on Ozone and Secondary Organic Aerosol, Chem. Rev., 113, 5848–5870, https://doi.org/10.1021/cr300520x, 2013.

Pollack, I. B., Ryerson, T. B., Trainer, M., Neuman, J. A., Roberts, J. M., and Parrish, D. D.: Trends in ozone, its precursors, and related secondary oxidation products in Los Angeles, California: A synthesis of measurements from 1960 to 2010, J. Geophys. Res. Atmos., 118, 5893–5911, https://doi.org/10.1002/jgrd.50472, https://agupubs.onlinelibrary.wiley.com/doi/abs/10.1002/jgrd.50472, 2013.

Praske, E., Crounse, J. D., Bates, K. H., Kurtén, T., Kjaergaard, H. G., and Wennberg, P. O.: Atmospheric Fate of Methyl Vinyl Ketone: Peroxy Radical Reactions with NO and HO_2, J. Phys. Chem. A, 119, 4562–4572, https://doi.org/10.1021/jp5107058, 2015.

Pusede, S. E., Gentner, D. R., Wooldridge, P. J., Browne, E. C., Rollins, A. W., Min, K.-E., Russell, A. R., Thomas, J., Zhang, L., Brune, W. H., Henry, S. B., DiGangi, J. P., Keutsch, F. N., Harrold, S. A., Thornton, J. A., Beaver, M. R., St. Clair, J. M., Wennberg, P. O., Sanders, J., Ren, X., VandenBoer, T. C., Markovic, M. Z., Guha, A., Weber, R., Goldstein, A. H., and Cohen, R. C.: On the temperature dependence of organic reactivity, nitrogen oxides, ozone production, and the impact of emission controls in San Joaquin Valley, California, Atmos. Chem. Phys., 14, 3373–3395, https://doi.org/10.5194/acp-14-3373-2014, 2014.

Pusede, S. E., Duffey, K. C., Shusterman, A. A., Saleh, A., Laughner, J. L., Wooldridge, P. J., Zhang, Q., Parworth, C. L., Kim, H., Capps, S. L., Valin, L. C., Cappa, C. D., Fried, A., Walega, J., Nowak, J. B., Weinheimer, A. J., Hoff, R. M., Berkoff, T. A., Beyersdorf, A. J., Olson, J., Crawford, J. H., and Cohen, R. C.: On the effectiveness of nitrogen oxide reductions as a control over ammonium nitrate aerosol, Atmos. Chem. Phys., 16, 2575–2596, https://doi.org/10.5194/acp-16-2575-2016, https://www.atmos-chem-phys.net/16/2575/2016/, 2016.

Pye, H. O. T., Luecken, D. J., Xu, L., Boyd, C. M., Ng, N. L., Baker, K. R., Ayres, B. R., Bash, J. O., Baumann, K., Carter, W. P. L., Edgerton, E. S., Fry, J. L., Hutzell, W. T., Schwede, D., and Shepson, P. B.: Modeling the Current and Future Roles of Particulate Organic Nitrates in the Southeastern United States, Environ. Sci. Technol., https://doi.org/10.1021/acs.est.5b03738, 2015.

Rindelaub, J. D., McAvey, K. M., and Shepson, P. B.: The photochemical production of organic nitrates from α-pinene and loss via acid-dependent particle phase hydrolysis, Atmos. Environ., 100, 193–201, https://doi.org/10.1016/j.atmosenv.2014.11.010, 2015.

Rollins, A. W., Browne, E. C., Min, K.-E., Pusede, S. E., Wooldridge, P. J., Gentner, D. R., Goldstein, A. H., Liu, S., Day, D. A., Russell, L. M., and Cohen, R. C.: Evidence for NO_x Control Over Nighttime SOA Formation, Science, 337, 1210–1212, https://doi.org/10.1126/science.1221520, http://www.sciencemag.org/content/337/6099/1210, 2012.

Romer, P. S., Duffey, K. C., Wooldridge, P. J., Allen, H. M., Ayres, B. R., Brown, S. S., Brune, W. H., Crounse, J. D., de Gouw, J., Draper, D. C., Feiner, P. A., Fry, J. L., Goldstein, A. H., Koss, A., Misztal, P. K., Nguyen, T. B., Olson, K., Teng, A. P., Wennberg, P. O., Wild,

R. J., Zhang, L., and Cohen, R. C.: The lifetime of nitrogen oxides in an isoprene-dominated forest, Atmos. Chem. Phys., 16, 7623–7637, https://doi.org/10.5194/acp-16-7623-2016, http://www.atmos-chem-phys.net/16/7623/2016/, 2016.

Romer, P. S., Duffey, K. C., Wooldridge, P. J., Edgerton, E., Baumann, K., Feiner, P. A., Miller, D. O., Brune, W. H., Koss, A. R., de Gouw, J. A., Misztal, P. K., Goldstein, A. H., and Cohen, R. C.: Effects of temperature-dependent NOx emissions on continental ozone production, Atmos. Chem. Phys., 18, 2601–2614, https://doi.org/10.5194/acp-18-2601-2018, https://www.atmos-chem-phys.net/18/2601/2018/, 2018.

Rosen, R. S., Wood, E. C., Wooldridge, P. J., Thornton, J. A., Day, D. A., Kuster, W., Williams, E. J., Jobson, B. T., and Cohen, R. C.: Observations of total alkyl nitrates during Texas Air Quality Study 2000: Implications for O_3 and alkyl nitrate photochemistry, J. Geophys. Res., 109, D07 303, https://doi.org/10.1029/2003JD004227, http://onlinelibrary.wiley.com/doi/10.1029/2003JD004227/abstract, 2004.

Russell, A. R., Valin, L. C., and Cohen, R. C.: Trends in OMI NO_2 observations over the United States: effects of emission control technology and the economic recession, Atmos. Chem. Phys., 12, 12 197–12 209, https://doi.org/10.5194/acp-12-12197-2012, 2012.

SEAC4RS Science Team: SEAC4RS field campaign data, NASA, https://www-air.larc.nasa.gov/cgi-bin/ArcView/seac4rs, 2014.

SOAS Science Team: SOAS 2013 Centreville site data, NOAA, https://esrl.noaa.gov/csd/groups/csd7/measurements/2013senex/Ground/DataDownload/, 2013.

Sobanski, N., Thieser, J., Schuladen, J., Sauvage, C., Song, W., Williams, J., Lelieveld, J., and Crowley, J. N.: Day and night-time formation of organic nitrates at a forested mountain site in south-west Germany, Atmos. Chem. Phys., 17, 4115–4130, https://www.atmos-chem-phys.net/17/4115/2017/acp-17-4115-2017.html, 2017.

Stelson, A. W. and Seinfeld, J. H.: Relative humidity and temperature dependence of the ammonium nitrate dissociation constant, Atmos. Environ., 16, 983–992, https://doi.org/10.1016/0004-6981(82)90184-6, http://www.sciencedirect.com/science/article/pii/0004698182901846, 1982.

Teng, A. P., Crounse, J. D., Lee, L., St. Clair, J. M., Cohen, R. C., and Wennberg, P. O.: Hydroxy nitrate production in the OH-initiated oxidation of alkenes, Atmos. Chem. Phys., 15, 4297–4316, https://doi.org/10.5194/acp-15-4297-2015, 2015.

Teng, A. P., Crounse, J. D., and Wennberg, P. O.: Isoprene Peroxy Radical Dynamics, J. Am. Chem. Soc., 139, 5367–5377, https://doi.org/10.1021/jacs.6b12838, 2017.

United States Environmental Protection Agency: Air Pollutant Emissions Trends Data, https://www.epa.gov/air-emissions-inventories/air-pollutant-emissions-trends-data, 2018.

Warneke, C., de Gouw, J. A., Holloway, J. S., Peischl, J., Ryerson, T. B., Atlas, E., Blake, D., Trainer, M., and Parrish, D. D.: Multiyear trends in volatile organic compounds in Los Angeles, California: Five decades of decreasing emissions, J. Geophys. Res. Atmos., 117, D00V17, https://doi.org/10.1029/2012JD017899, https://agupubs.onlinelibrary.wiley.com/doi/abs/10.1029/2012JD017899, 2012.

Wennberg, P. O., Bates, K. H., Crounse, J. D., Dodson, L. G., McVay, R. C., Mertens, L. A., Nguyen, T. B., Praske, E., Schwantes, R. H., Smarte, M. D., St Clair, J. M., Teng, A. P., Zhang, X., and Seinfeld, J. H.: Gas-Phase Reactions of Isoprene and Its Major Oxidation Products, Chem. Rev., 118, 3337–3390, https://doi.org/10.1021/acs.chemrev.7b00439, https://doi.org/10.1021/acs.chemrev.7b00439, 2018.

Xiong, F., Borca, C. H., Slipchenko, L. V., and Shepson, P. B.: Photochemical degradation of isoprene-derived 4,1-nitrooxy enal, Atmos. Chem. Phys., 16, 5595–5610, https://doi.org/10.5194/acp-16-5595-2016, 2016.

Xu, L., Guo, H., Boyd, C. M., Klein, M., Bougiatioti, A., Cerully, K. M., Hite, J. R., Isaacman-VanWertz, G., Kreisberg, N. M., Knote, C., Olson, K., Koss, A., Goldstein, A. H., Hering, S. V., Gouw, J. d., Baumann, K., Lee, S.-H., Nenes, A., Weber, R. J., and Ng, N. L.: Effects of anthropogenic emissions on aerosol formation from isoprene and monoterpenes in the southeastern United States, Proc. Natl. Acad. Sci. USA, 112, 37–42, https://doi.org/10.1073/pnas.1417609112, http://www.pnas.org/content/112/1/37, 2015a.

Xu, L., Suresh, S., Guo, H., Weber, R. J., and Ng, N. L.: Aerosol characterization over the southeastern United States using high-resolution aerosol mass spectrometry: spatial and seasonal variation of aerosol composition and sources with a focus on organic nitrates, Atmos. Chem. Phys., 15, 7307–7336, https://doi.org/10.5194/acp-15-7307-2015, https://www.atmos-chem-phys.net/15/7307/2015/, 2015b.

Zare, A., Romer, P. S., Nguyen, T., Keutsch, F. N., Skog, K., and Cohen, R. C.: A comprehensive organic nitrate chemistry: insights into the lifetime of atmospheric organic nitrates, Atmos. Chem. Phys., 18, 15 419–15 436, https://doi.org/10.5194/acp-2018-530, 2018.